Characterization and use of a lignin sample extracted from Eucalyptus grandis sawdust for the removal of methylene blue dye

Alexandra Cemin, Fabrício Ferrarini, Matheus Poletto, Luis R Bonetto, Jordana Bortoluz, Laurent Lemée, Régis Guégan, Valdemar I Esteves, Marcelo Giovanela

Characterization and use of a lignin sample extracted from Eucalyptus grandis sawdust for the removal of methylene blue dye

Alexandra Cemin, Fabrício Ferrarini, Matheus Poletto, Luis R. Bonetto, Jordana Bortoluz, Laurent Lemée, Régis Guégan, Valdemar I. Esteves, Marcelo Giovanela

PII: S0141-8130(20)35329-0

DOI: https://doi.org/10.1016/j.ijbiomac.2020.12.155

Reference: BIOMAC 17535

To appear in: *International Journal of Biological Macromolecules*

Received date: 7 September 2020

Revised date: 7 December 2020

Accepted date: 19 December 2020

Please cite this article as: A. Cemin, F. Ferrarini, M. Poletto, et al., Characterization and use of a lignin sample extracted from Eucalyptus grandis sawdust for the removal of methylene blue dye, *International Journal of Biological Macromolecules* (2020), https://doi.org/10.1016/j.ijbiomac.2020.12.155

Characterization and use of a lignin sample extracted from *Eucalyptus grandis* sawdust for the removal of methylene blue dye

Alexandra Cemin[a], Fabrício Ferrarini[b], Matheus Poletto[a], Luis R. Bonetto[a], Jordana Bortoluz[a], Laurent Lemée[c], Régis Guégan[d,e], Valdemar I. Esteves[f], Marcelo Giovanela[a,*]

[a] *Área do conhecimento de Ciências Exatas e Engenharias, Universidade de Caxias do Sul, Rua Francisco Getúlio Vargas, 1130, Caxias do Sul, 95070-560, RS, Brazil*

[b] *Laboratório Virtual de Predição de Propriedades – LVPP, Departamento de Engenharia Química, Universidade Federal do Rio Grande do Sul, Rua Ramiro Barcelos, 2777, Bairro Santana, Porto Alegre, 90035-007, RS, Brazil*

[c] *Institut de Chimie des Milieux et Matériaux de Poitiers (IC2MP CNRS UMR 7285), Université de Poitiers, 4 rue Michel Brunet – TSA 51106, 86073 Poitiers Cedex 09, France*

[d] *Institut des Sciences de la Terre d'Orléans, UMR 7327, CNRS - Université d'Orléans, 1A rue de la Férollerie, 45071 Orléans Cedex 2, France*

[e] *Faculty of Science and Engineering, Global Center for Science and Engineering, Waseda University, 3-4-1 Okubo, Shinjuku-ku, Tokyo, 169-8555, Japan*

[f] *CESAM - Centre for Environmental and Marine Studies, Department of Chemistry, University of Aveiro, Campus de Santiago, 3810-193, Aveiro, Portugal*

* Corresponding author. Tel.: +55 54 322182100. E-mail: mgiovan1@ucs.br (M. Giovanela)

1. Introduction

The amount of pollutants generated by industry has grown exponentially worldwide over the past years [1]. This problem is of major concern, especially when related to water contamination, since all forms of life depend on water resources [2]. Additionally, the textile industry is one of the industries with the highest water consumption: on average, approximately 125 L of wastewater is generated per textile processing unit [3–5]. Furthermore, natural and synthetic dyes are predominantly used by this industry and, therefore, are primarily responsible for the pollution of the water used in its finishing processes [6]. Annually, approximately 2 to 3% of these dyes enter the wastewater from this sector [7].

Concern regarding the disposal of textile wastewater without previous treatment into aquatic environments was one of the main motivations of this study since such wastewater can quickly lead to the depletion of dissolved oxygen, thereby resulting in an oxygen imbalance in these ecosystems [8,9]. The presence of dyes in water bodies also prevents the penetration of sunlight, thereby altering the photosynthetic activity of the environment, which results in the deterioration of the water quality and, consequently, in adverse effects on the local fauna and flora [10,11].

In an attempt to minimize the impacts that result from the inappropriate disposal of these substances into the environment, in the last decades, the search for new forms of treatment has intensified considerably [1,10,12]. Currently available techniques for the treatment of textile wastewater must be improved, and it is highly necessary to develop and implement alternative methodologies that are efficient and economically viable [12].

Numerous methods are available for treating wastewater that contains dyes. Despite the availability of many techniques for removing dye contaminants from wastewaters, such as coagulation, chemical oxidation, membrane separation processes, electrochemical techniques, and aerobic and anaerobic microbial degradation, each of these methods has inherent limitations [10,13]. The disadvantages of these methods include low removal efficiency, high production of sewage sludge, generation of toxic by-products, and the use of more potentially toxic chemicals. In this context, the adsorption technique has been found to be the most effective and economical process, especially when by-products of other productive processes are employed as adsorbents [2,14].

In recent years, significant attention has been focused on adsorbent materials derived from lignin. This biopolymer is one of the main by-products of the cellulose industry and the second most abundant substance in nature (its content in wood ranges from 20 to 30% on a

dry basis). Although the molecular structure of lignin is very complex, it is known to contain several oxygenated functional groups such as alcoholic and phenolic hydroxyl groups and methoxyl groups. These functional groups can bind metal ions, pharmaceuticals and dye molecules by physicochemical interactions, which include ion exchange and complexation [15–18]. Hence, this material (in its natural or modified form) has been frequently used for the remediation of wastewater that contains dyes [7].

The chemical structure of lignin has distinctive characteristics, which depend on the origin and growing conditions of the plant. The processes used to obtain the lignin also greatly influence its final structure and properties [19]. Since naturally occurring lignin cannot be isolated in its unaltered form, several methods have been used to separate it from the other lignocellulosic materials of wood via physical and/or chemical techniques. In these methods, lignin is usually recovered as an insoluble residue, a derivative or an extract/liquor. In the Klason method, for example, the lignin is released as an insoluble residue after hydrolysis and solubilization of the samples with 72% sulfuric acid. In the isolation of the lignin as a derivative, soluble products are released during treatment with chemicals, and these products are separated at the end of the reaction. As an extract/liquor, organic solvents such as dioxane and water or acetone and water are used to obtain lignin [20].

According to some studies, only 5% of the available lignin is utilized worldwide. Hence, significant opportunities remain for developing advanced engineering materials with this compound and for identifying possible applications in its natural form [7,21]. There are several published reports in the literature on the extraction and characterization of lignins from vegetable biomasses. Two examples are the studies of Watkins et al. [22] and Naron et al. [23]. However, the data available on lignins from *Eucalyptus* remain highly scarce, especially in relation to their application in adsorption processes that involve dyes.

Even in this context, the influence of the experimental parameters, such as the adsorbent dosage, pH and stirring frequency, on the adsorption capacity of these materials is not discussed extensively in the literature. In most studies, modifications are made to the structure of the lignocellulosic materials using various methods with strong oxidizing agents and other chemicals for their subsequent application almost exclusively in the removal of metals from aqueous solutions, while dye adsorption is covered by few studies.

Suteu et al. [24], for example, evaluated the removal of a reactive dye, namely, Brilliant Red HE-3B, using industrial lignin. These authors found that the monolayer sorption capacity of industrial lignin was 10.173 mg g^{-1} and that this material was promising as a sorbent for reducing the pollution of textile wastewater. Zhang et al. [25] used organosolv

lignin from rice straw to remove methylene blue (MB) dye from water. In this study, the authors found that the monolayer capacity of this material was 40 mg g^{-1}. Moreover, they demonstrated that the MB removal performance depends strongly on the pH value. Li et al. [26] investigated lignin-based hydrogels for the removal of cationic dyes. These authors showed that this adsorbent for MB dye removal showed a fivefold increase in capacity, namely, to 495 mg g^{-1} at 30 °C, compared to raw lignin (kraft lignin).

In consideration of these results, the extraction of lignin from wood sawdust of the furniture industry has proved to be convenient since this sector generates a large amount of waste that rarely has an ecologically suitable destination and, therefore, can cause several problems to the environment [27,28]. Various positive results for the use of this material as an adsorbent have been reported [7]. In addition, we chose to work with sawdust of the *E. grandis* species because it is the most planted tree in the Brazilian territory (308,500 ha of planted area) [29] and the most frequently used material in furniture manufacturing.

Therefore, the main objectives of this study were *(i)* to extract lignin from *E. grandis* sawdust, *(ii)* to characterize the extracted lignin via several analytical tools, and *(iii)* to evaluate its possible application as an adsorbent for the removal of MB dye from aqueous solutions by adsorption.

2. Materials and methods

2.1 Materials

E. grandis sawdust was collected at Madeireira Peretto Material de Construção, which is located in the municipality of Caxias do Sul (Rio Grande do Sul state, southern Brazil), and this sawdust was generated from the cutting of logs without any type of previous treatment. The wood sawdust used in this study contains approximately 32 wt. % of lignin. Detailed information regarding this sawdust has been previously published elsewhere [30].

MB dye ($C_{16}H_{18}ClN_3S \cdot 3H_2O$, Color Index 52015) was purchased from Vetec Química Fina, while the chemical reagents (KNO_3, KOH, HNO_3, HCl and NaOH) were of analytical grade and commercially obtained from Sigma-Aldrich (São Paulo, Brazil). All aqueous solutions were prepared with deionized water obtained from a Millipore Direct-Q 3 UV system (Darmstadt, Germany).

2.2 Lignin extraction

Klason lignin was extracted from the *E. grandis* sawdust using the T222 om-93 method, which was proposed by the Technical Association of the Pulp and Paper Industry (TAPPI). The sawdust was sieved and subjected to three consecutive washes to remove the main extractives from the sawdust. The first wash was conducted with a mixture of ethanol/benzene (2:1, v/v), the second with ethanol, and the last with distilled water. For this, the sawdust was packed in a cellulose cartridge and placed in a Soxhlet with a condenser.

These washes were carried out using temperatures close to the boiling points of the solvents with the aid of a heating blanket. To avoid the loss of solvent by evaporation, the system was connected to a thermostated water bath at 15 °C, which kept the system cool throughout the entire extraction procedure. The extraction time for each solvent was 4 h, and the time interval started after the first extraction cycle.

After these three washes, the material (approximately 1.0 g of sawdust without extractives) was transferred to another flask that contained an aqueous solution of sulfuric acid (72%, v/v), where it remained under reflux for 4 h. Then, the lignin was washed with distilled water using vacuum filtration until the pH of the filtrate was close to neutral. Finally, the lignin was dried in an oven at 70 °C for 4 h and stored in a desiccator until the analyses. The lignin content was determined based on the oven-dry weight of sawdust, according to the method mentioned above. Prior to the adsorption tests, the extracted lignin was ground in an agate mortar using a pestle to standardize the size of the particles.

2.3 Lignin characterization

2.3.1 Elemental analysis

The mass percentages of carbon, hydrogen, nitrogen, and sulfur in the *E. grandis* lignin sample were determined in an elemental analyser TRUSPEC 630-200-200 at the University of Aveiro (Portugal). The mass percentage of oxygen was obtained by calculating the following difference: [% O = 100% – (% C +% H +% N +% S)].

2.3.2 Fourier transform infrared (FT-IR) spectroscopy

The main functional groups in the structure of the *E. grandis* lignin sample were identified by Fourier transform infrared (FT-IR) spectroscopy. A spectrum with 1,024 scans was recorded on a NICOLET iS10 spectrophotometer with a nominal resolution of 4 cm^{-1} and within the spectral range of 4,000 to 400 cm^{-1}.

2.3.3 Solid-state ^{13}C nuclear magnetic resonance (^{13}C NMR) spectroscopy

The ^{13}C NMR spectrum of the *E. grandis* lignin in the solid state was obtained at the University of Aveiro (Portugal) in a BRUKER AVANCE III 400 MHz spectrometer operating with a magnetic field of the order of 9.4 T. The sample (~ 100 mg) was initially packaged in a 4 mm diameter rotor. The spectrum was recorded using the cross-polarization technique with a contact time of 2,000 μs and a rotation of the magic angle of 12 kHz. The time between two consecutive pulses was 5 s, and the acquisition time was 15 ms.

2.3.4 Pyrolysis coupled to gas chromatography interfaced with mass spectrometry (Py-GC/MS)

The *E. grandis* lignin sample was pyrolysed using a FRONTIER LAB EGA 2020 pyrolyser equipped with an AS-1020E sampler coupled to a gas chromatograph and a quadrupolar mass analyser from SHIMADZU (QP 2010 Ultra) at Université de Poitiers (France). The sample (~ 5 mg) was treated with 10 μL of a solution of tetramethylammonium hydroxide (TMAH) in methanol (50:50 v/v) in a stainless-steel cup and pyrolysed at 350 °C for 1 min.

The pyrolysis products (pyrolysates) were introduced using an injector at 250 °C with a continuous and constant flow of helium gas of 1 mL min^{-1}. The chromatographic separation was conducted on a Supelco SLB-5MS capillary column (30 m × 0.25 mm i.d. and 0.25 μm phase thickness). The column temperature was increased from 50 to 300 °C at a rate of 5 °C min^{-1} and maintained at 300 °C for 9 min. The ionization mode was electron impact (70 eV), and the source temperature was 220 °C.

The main products of the pyrolysed lignin sample were identified based on their retention times (t_R) and by comparison of their mass spectra with those reported in the literature and with spectra from the National Institute of Standards and Technology (NIST) data library.

2.3.5 Field-emission scanning electron microscopy (FESEM)

The morphology of the *E. grandis* lignin sample was evaluated using the field-emission scanning electron microscopy (FESEM) technique. Prior to the analysis, the material was sputtered with a thin layer of gold for 3 min. Then, images were obtained using a TESCAN MIRA3 electron microscope that operated with a 20 kV electron beam.

2.3.6 Thermogravimetric analysis (TGA)

The thermal stability of the *E. grandis* lignin sample was evaluated in a SHIMADZU TGA-50 thermogravimetric analyser. The sample (~ 10 mg) was analysed under an inert atmosphere of N_2 with a flow of 50 mL min^{-1} using a platinum sample holder heated from 25 to 900 °C at a heating rate of 10 °C min^{-1}.

2.3.7 Specific surface area and pore size

The specific surface area and the pore size of the *E. grandis* lignin sample were determined using the Brunauer, Emmett and Teller (BET) and the Barret, Joyner and Halenda (BJH) methods at the Université d'Orléans (France) in a NOVA surface area analyser from QUANTACHROME INSTRUMENTS. Approximately 150 mg of the sample was maintained at 150 °C under vacuum (~ 1×10^{-3} mbar) for 24 h to remove moisture and other volatile compounds that could possibly be adsorbed on the surface of the sample. The adsorption and desorption isotherms of N_2 by the sample at 77 K were obtained using relative vapour pressures (P/P_0) from 0.0116 to 0.0984. The average area occupied by an N_2 molecule to form a complete monolayer was assumed to be 16.2 Å².

2.3.8 pH at the zero-charge point (pH_{PZC})

The pH at the zero charge point (pH_{PZC}) was determined by the batch equilibrium method, which was adapted from Smiciklas [31]. Approximately 100 mg of the *E. grandis* lignin sample was transferred to several Erlenmeyer flasks with a capacity of 100 mL that contained 50 mL of a 0.1 mol L^{-1} KNO_3 solution. The pH values were adjusted in the range of 2.0 to 11.0 by adding 0.1 mol L^{-1} KOH or HNO_3 solutions. The suspensions remained under constant stirring at a frequency of 150 rpm on an incubator shaker for 480 min at a controlled temperature of 25 °C. At the end of this procedure, all samples were filtered, and the initial and final pH values were measured on a DIGIMED DM-20 pH meter (São Paulo, Brazil).

2.4 Adsorption experiments

The influence of the experimental parameters (lignin dosage: 50, 75, 100, 125, 150, 175, 200, 225, 250 and 300 mg; stirring frequency: 90, 120, 150, 180, 210 and 250 rpm; and initial pH: 2.0 to 11.0 in increments of unity) on the adsorption process was evaluated in terms of two response variables: the adsorption capacity of the MB by the *E. grandis* lignin sample (q_t, mg g^{-1}) and the percentage of MB removal (*%R*).

These variables were calculated using **Equations (1)** and **(2)**, respectively [32]:

$$q_t = \frac{(C_0 - C_t)}{m} \cdot V \quad \textbf{(1)}$$

$$\%R = \frac{(C_0 - C_t)}{C_0} \cdot 100 \quad \textbf{(2)}$$

where q_t is the amount of MB retained per gram of lignin as a function of time (mg g^{-1}); C_0 and C_t are the initial concentration and the concentration at time t, respectively, of MB (mg L^{-1}); V is the volume of the dye solution (L), and m is the mass of the lignin (g).

The adsorption equilibrium was evaluated using the optimum values obtained in the preliminary tests by varying the initial concentration of dye in the range of 50 to 150 mg L^{-1} in intervals of 25 mg L^{-1}. Isotherms were constructed from the analysis of the interaction between the adsorption capacity at equilibrium and the final concentration of MB, and at equilibrium at 25 °C and a contact time of 8 h. The obtained experimental data were adjusted according to the isothermal models of Freundlich [33], Langmuir [34], and Temkin and Dubinin-Radushkevich [32], all in their non-linear forms.

The expression proposed by Freundlich is presented as **Equation (3)**:

$$q_e = k_F C_e^{1/n} \quad \textbf{(3)}$$

where k_F (mg g^{-1} (mg L^{-1})$^{-1/n}$) and n are constants that depend on the temperature and are related to the adsorption capacity and intensity, respectively.

The expression proposed by Langmuir is presented as **Equation (4)**:

$$q_e = \frac{q_m k_L C_e}{1 + k_L C_e} \quad \textbf{(4)}$$

where C_e represents the concentration of MB at equilibrium (mg L^{-1}), q_e is the amount of MB adsorbed per unit mass of the adsorbent at equilibrium (mg g^{-1}), q_m is the maximum theoretical adsorption capacity that corresponds to a monolayer covering (mg g^{-1}), and k_L is the Langmuir isothermal constant (L mg^{-1}).

The separation factor (R_L) can be used to evaluate the adsorption process. The meaning of this parameter is described in **Table 1,** and it can be defined according to **Equation (5)** [32]:

$$R_L = \frac{1}{1 + k_l C_0} \quad \textbf{(5)}$$

Table 1. Separation factor and types of isotherms

Classification	Isotherm type
$R_L > 1$	Unfavourable
$R_L = 1$	Linear
$0 < R_L < 1$	Favourable
$R_L = 0$	Irreversible

The expression proposed by Temkin is presented as **Equation (6):**

$$q_e = \frac{RT}{b_t} \ln(A_t C_e) \quad \textbf{(6)}$$

where C_e represents the concentration of MB at equilibrium (mg L^{-1}), q_e is the amount of MB adsorbed per unit mass of lignin at equilibrium (mg g^{-1}), A_t is the equilibrium binding constant (L mg^{-1}) that corresponds to the maximum binding energy, b_t is the maximum theoretical heat of adsorption (J mol^{-1}), R is the universal gas constant (8.314 J K^{-1} mol^{-1}), and T is the temperature (K).

The expression proposed by Dubinin-Radushkevich is presented as **Equation (7):**

$$q_e = q_s \exp^{(k_{ad}\epsilon)} \quad \textbf{(7)}$$

The parameter ∈ is calculated by **Equation (8):**

$$\epsilon = RT \ ln \ (1 + \frac{1}{C_e}) \quad \textbf{(8)}$$

where q_s is the adsorption capacity (mg g^{-1}), k_{ad} is a constant related to the sorption energy (mol^2 J^{-2}), ∈ is the Polanyi potential (kJ mol^{-1}), R is the gas constant (8.314 J K^{-1} mol^{-1}) and T is the temperature (K).

The adsorption kinetics were evaluated using two models, namely, a pseudo-first-order (PFO) model [35] and a pseudo-second-order (PSO) model [36], which are presented in **Equations (9)** and **(10)**, respectively:

$$q_t = q_e(1 - e^{-k_1 t}) \quad \textbf{(9)}$$

$$q_t = \frac{q_e^2 \, k_2 \, t}{1 + k_2 \, q_e \, t} \quad \textbf{(10)}$$

where q_e and q_t are the amounts of MB retained per gram of lignin at equilibrium and at time t (mg g^{-1}), respectively; k_1 is the pseudo-first-order kinetic constant (min^{-1}) and k_2 is the pseudo-second-order kinetic constant (g $mg^{-1}min^{-1}$).

The parameters of the models (equilibrium and kinetic) that minimized the objective function (F_{obj}) were estimated using the Microsoft Excel Solver tool. F_{obj} was defined as the mean square error of the amount of retained MB per gram of lignin, as expressed in **Equation (11)** was used. This function represents the difference between the experimental values and those calculated by the model. Hence, the lower its value, the more accurate the model is, and the better the behaviour of the experimental data are described. Thus, during parameter estimation, F_{obj} is minimized to identify the optimal parameter values.

$$F_{obj} = \frac{1}{NP} \sum_{i=1}^{NP} \left(q_i^{exp.} - q_i^{calc.}\right)^2 \quad \textbf{(11)}$$

In the above equation, NP is the number of experimental points, and $q_i^{exp.}$ and $q_i^{calc.}$ represent the experimental adsorption capacity and that calculated by the model (mg g^{-1}). In addition, the models were compared statistically using the Fisher test (F). In this test, the variance is calculated for each of the models to be compared (σ_i^2 and σ_j^2) using the F_{obj} value obtained in the parameter estimation and their respective degrees of freedom (DF). The degrees of freedom represent the differences between the number of experimental points and the number of parameters (N_{pars}) in the model. Then, the F value is obtained by calculating the ratio between the variances of the models to be compared according to **Equation (12)**:

$$F = \frac{\sigma_i^2}{\sigma_j^2} = \frac{\frac{F_{obj,i}}{DF_i}}{\frac{F_{obj,j}}{DF_j}} = \frac{\frac{F_{obj,i}}{NP_i - N_{pars,i}}}{\frac{F_{obj,i}}{NP_j - N_{pars,j}}} \quad \textbf{(12)}$$

This test determines whether there is a significant difference between the models when the confidence is 95% and ($NP - N_{pars}$) degrees of freedom are considered. If the F value is within the maximum and minimum limits of Fisher's F distribution (F_{max} and F_{min}), the hypothesis of statistical equality between the models is supported [37].

In addition, to select the model that best fits the set of experimental data, the values of the coefficient of determination (R^2), which is defined in **Equation (13)**, were also considered:

$$R^2 = 1 - \frac{\sum_{i=1}^{n}\left(y_{i\,mod} - y_{i\,exp}\right)^2}{\sum_{i=1}^{n}\left(y_{i\,exp} - \overline{y_{i\,exp}}\right)^2} \quad \textbf{(13)}$$

where $y_{i\,exp}$ are the experimentally observed values and $\overline{y_{i\,exp}}$ is the observed experimental average of the n experimental data [38].

The thermodynamic parameters were determined under the same experimental conditions as those used to assess the equilibrium and kinetics of the adsorption process, except for the C_0 factor, for which only the value of 100 mg L^{-1} was used. The values of $\Delta G°_{ads}$ and k_C were determined through the direct application of **Equations (14)** and **(15)**, respectively, while $\Delta H°_{ads}$ and $\Delta S°_{ads}$ were obtained from the angular and linear coefficients, respectively, by applying the method of linear regression to the van't Hoff equation (**Equation (16)**):

$$\Delta G^{\circ}_{ads} = -RT\,ln\,k_e \quad \textbf{(14)}$$

$$k_c = \frac{C_0 - C_e}{C_e} \quad \textbf{(15)}$$

$$ln\,k_e = \frac{-\Delta H^{\circ}_{ads}}{RT} + \frac{\Delta S^{\circ}_{ads}}{R} \quad \textbf{(16)}$$

where R is the ideal gas constant (8.314 J mol^{-1} K^{-1}), T is the temperature (K), k_c is the equilibrium constant and C_0 (mg L^{-1}) and C_e (mg L^{-1}) represent the initial MB concentration and the concentration of MB at equilibrium, respectively, in the solution.

To evaluate the reuse of *E. grandis* lignin, after the MB adsorption, four cycles of desorption/adsorption were conducted. Each cycle consisted an adsorption test, followed by washing with Milli-Q water (desorption), since materials from waste from plant sources cannot be recovered by methods that involve excessive heat. The use of acidic or basic solutions, along with pure solvents, such as methanol, ethanol and acetone, was avoided in this final step of this work to make the process more environmentally friendly (by minimizing waste and using a non-toxic solvent).

At the end of the first adsorption test, the Erlenmeyer contents were filtered and washed with five 100 mL portions of Milli-Q water. Then, the lignin sample retained in the filter paper was dried in an oven at 70 °C for 12 h. The adsorption, with the regenerated material, was carried out four additional times, and the removal percentages were compared with the percentage obtained the first time. All of these tests were performed in duplicate based on the previously optimized experimental parameters.

3. Results and discussion

3.1 Lignin characterization

3.1.1 Preliminary considerations

The Klason method used in the present work proved to be efficient, robust and relatively inexpensive. Moreover, the extraction percentage was approximately 26 wt. %, and the average cost of isolating of this material from the *E. grandis* sawdust was approximately US$ 20.8 per gram. The extraction percentage found here was similar to others values described in the literature. Xiao et al. [39], for example, reported a content of 26.9 wt. % for a lignin extracted from an *E. urophylla* × *E. grandis* clonal hybrid, while Salem et al. [40] found a content of 27.9 wt. % for a lignin isolated from *E. grandis*. Concerning the particle size, the lignin sample consists of fragments with an average diameter of approximately 1.15 ± 0.18 mm.

3.1.2 Elemental analysis

The elemental composition of the *E. grandis* lignin sample is presented in **Table 2**. Carbon and oxygen are present in larger mass proportions in the material, which may be indicative of the presence of several oxygenated functional groups in the structure of lignin. The values reported here are very similar to those that have been obtained for samples of

lignins from pulp mills in South Africa and other lignins, such as *Pinus* [23]. These percentages are also similar to those obtained by other authors who analysed *Eucalyptus* species [41,42].

Table 2. Results of the elemental analysis for *E. grandis* lignin

Element	Mass percentage (%)
C	57.66
H	5.09
N	0.11
S	0.32
O	36.82

3.1.3 Fourier transform infrared (FT-IR) spectroscopy

Figures 1 shows the FT-IR spectra of the *E. grandis* lignin sample **(a)** before and **(b)** after MB adsorption, and the assignments of the main peaks in the FT-IR spectrum of **Figure 1a** are summarized in **Table 3**.

Figure 1. FT-IR spectra of the *E. grandis* lignin **(a)** before and **(b)** after MB adsorption

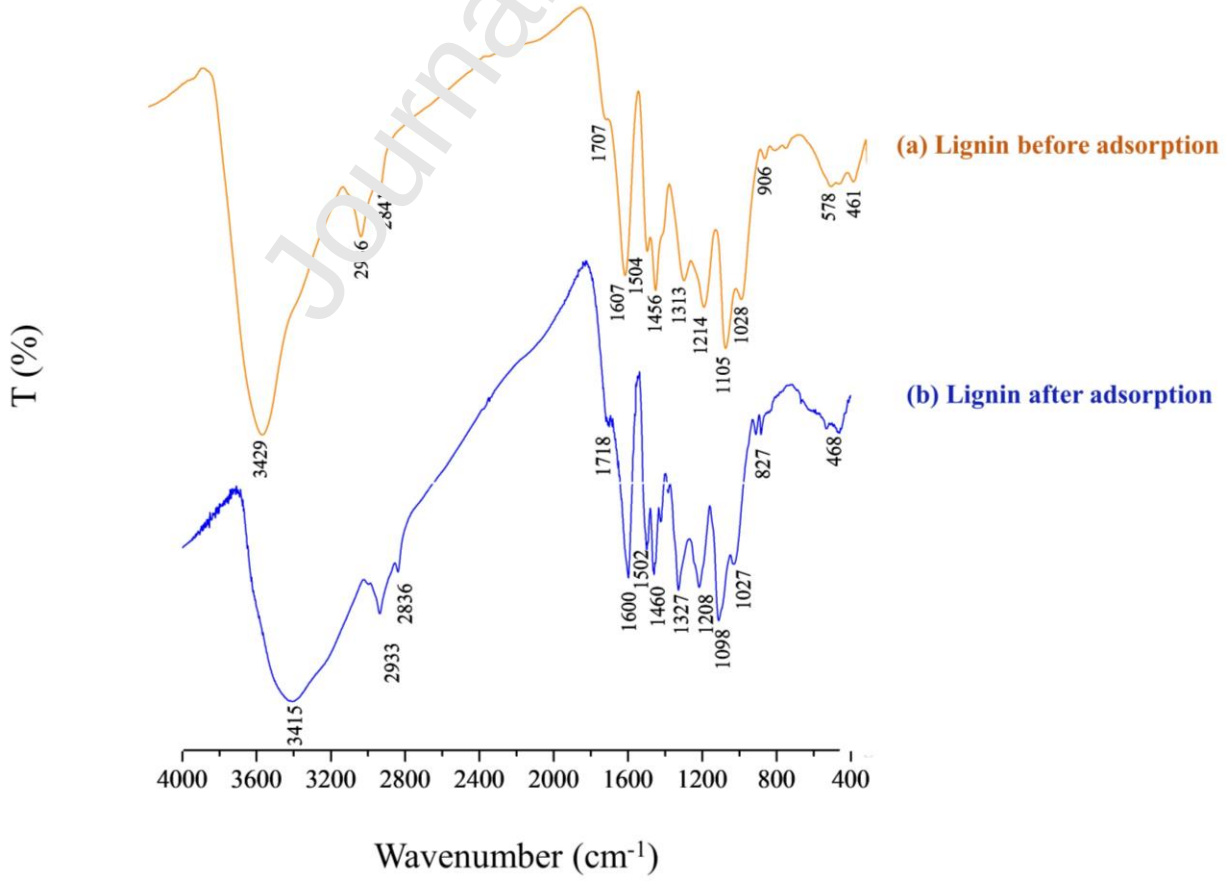

Table 3. Assignments of the main peaks in the FT-IR spectrum of the *E. grandis* lignin before MB adsorption [20,43,44]

Wavenumbers (cm^{-1})	Functional groups
3429	Stretching vibration of O-H groups
2936 and 2841	Asymmetric and symmetric stretching of aliphatic C-H
1707	C=O stretching of carboxylic acids, ketones, and aldehydes
1607 and 1504	Aromatic ring vibration
1456	Asymmetric deformation of aliphatic C-H
1313	Axial C-O deformation of syringe and/or guaiacyl units
1214	Aromatic C-O stretching
1028	C-H deformation in the plane in guaiacyl units and C-O in secondary alcohols and aliphatic ethers
906, 578 and 461	Deformation of aliphatic and aromatic C-H outside the plane

The axial and angular deformations identified in the FT-IR spectrum of the *E. grandis* lignin sample (**Figure 1a**) are mostly similar to those reported by Piló-Veloso [20], Morais et al. [43] and Saliba et al. [44]. Moreover, comparable FT-IR spectra were obtain in other study, e.g., of modified sugarcane bagasse lignin and *Shorea robusta* lignin [45,46]. Hence, although these lignins come from different sources, the functional groups present in the chemical structures of these materials are similar.

All these functional groups can interact with the MB molecules during the adsorption process. This can be observed in **Figure 1b**. Although some peaks have shifted to smaller wavenumbers or their intensities have changed, both spectra show similar characteristics. However, after MB adsorption, the peaks at 1502 and 1327 cm^{-1} increased in intensity, thereby demonstrating that the aromatic and C-O groups participate more directly in the removal. Similar results have been reported in other studies that also used vegetable biomasses to remove MB dye [47–49].

3.1.4 Solid-state ^{13}C nuclear magnetic resonance (^{13}C NMR) spectroscopy

A solid-state ^{13}C NMR spectrum of the *E. grandis* lignin sample is shown in **Figure 2**. The ^{13}C NMR spectrum presents the main characteristic signals for the lignin. These results are supported by the FT-IR analysis since the identified peaks are directly correlated with the functional groups identified in the FT-IR spectrum.

Figure 2. Solid-state ^{13}C NMR spectrum of *E. grandis* lignin

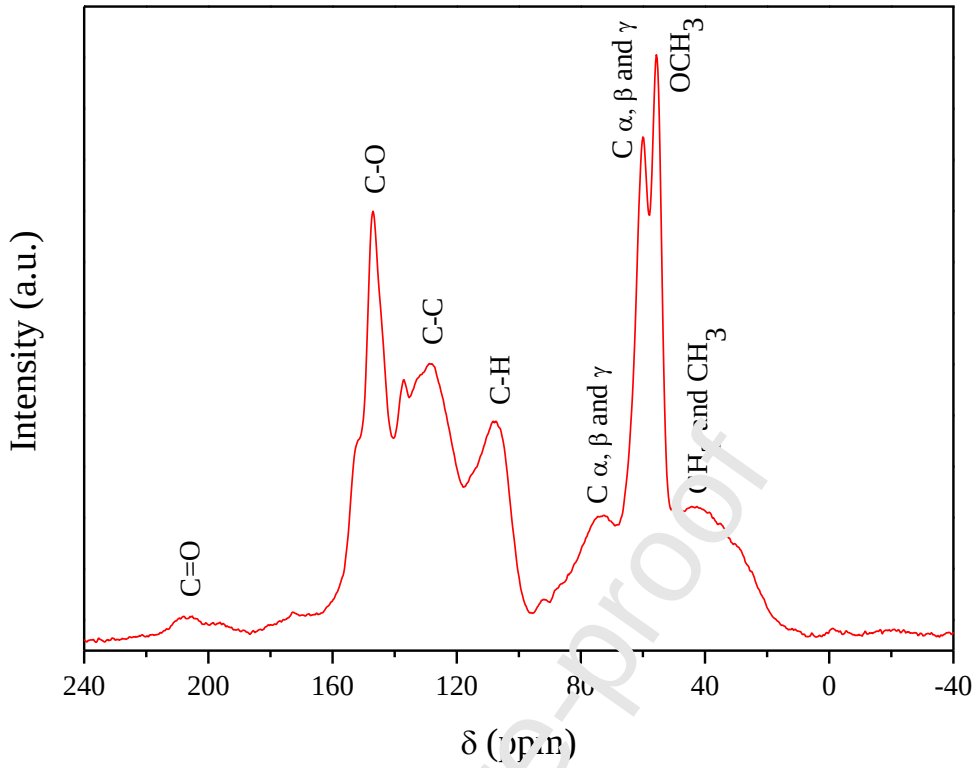

In the region that corresponds to aliphatic carbons (100 to 20 ppm), a low-intensity signal at 43 ppm is observed, which is attributed to CH_2-type carbons and possibly CH_3-type carbons of saturated aliphatic chains. In addition, the region at 55 ppm shows a very intense peak, which is characteristic of the methoxyl group (OCH_3) [19]. Additionally, in this region (from 60 to 95 ppm), signals related to α, β and γ aliphatic carbons are observed, which are related to chemical bonds β-O-4, α-O-4, β-β and β-5 [50–52]. Regarding the aromatic carbon region (160 to 100 ppm), the signals observed at 107, 128, 137 and 147 ppm are characteristic of guaiacyl units. Syringyl units can be identified between 152 and 154 ppm [53]. Finally, the spectrum shows a very discrete peak at 207 ppm, which corresponds to a low incidence of carbonyl carbon atoms in the chemical structure of *E. grandis* lignin [19].

3.1.5 Pyrolysis coupled to gas chromatography interfaced with mass spectrometry (Py-GC/MS)

Twenty compounds were identified by GC-MS (**Table 4**) in the pyrogram of the *E. grandis* lignin sample (**Figure 3**). These compounds were mainly phenolic moieties that are characteristic of lignocellulosic materials [54,55]. The ubiquitous palmitic (C_{16}) and stearic (C_{18}) fatty acid methyl esters, which are not specific, were also detected.

Figure 3. Pyrogram of *E. grandis* lignin

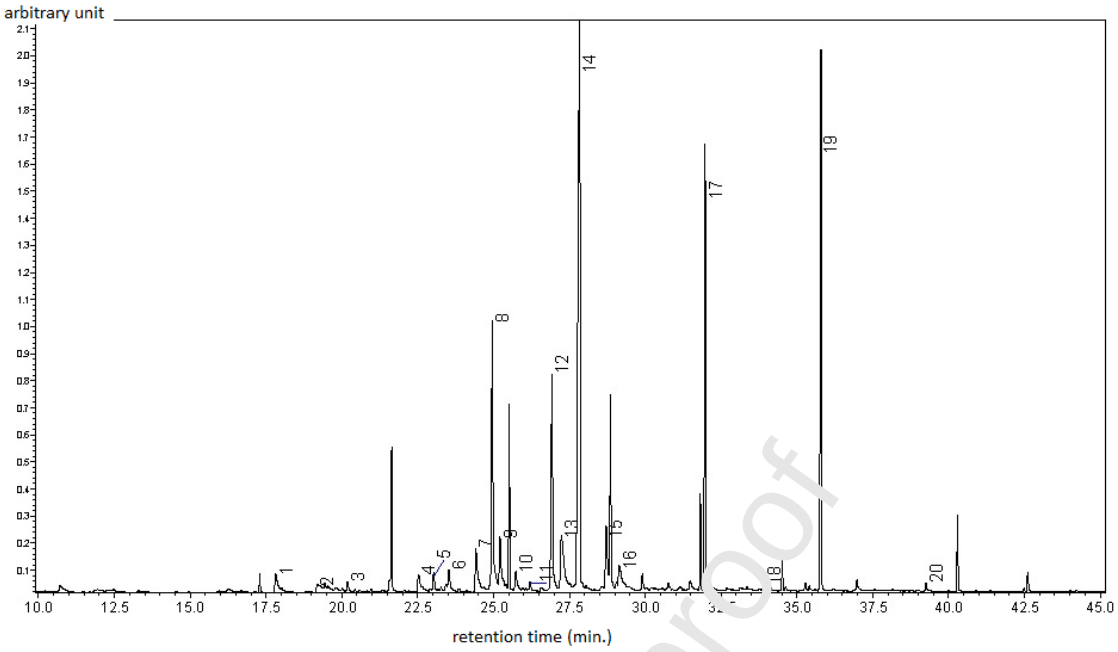

Table 4. Pyrolysis products identified in the pyrogram of *E. grandis* lignin

Peak #	Compound	Retention time (min)
1	trimethoxy benzene	17.8
2	dimethoxy phenol	19.2
3	trimethoxy methylbenzene	20.2
4	dimethoxy benzaldehyde	22.5
5	dimethoxy (2-methoxyethenyl)benzene	23.0
6	tetramethoxy benzene	23.5
7	dimethoxy acetophenone	24.4
8	dimethoxy benzoic acid methyl ester	24.9
9	trimethoxy benzaldehyde	25.2
10	dimethoxy benzeneacetic acid methyl ester	25.7
11	trimethoxy propenylbenzene	26.2
12	trimethoxy acetophenone	26.9
13	trimethoxy benzoic acid	27.2
14	trimethoxy benzoic acid methyl ester	27.8
15	trimethoxyphenyl propionic acid	28.7
16	trimethoxy benzyl methyl ether	29.2
17	hexadecanoic acid, methyl ester	31.9
18	heptadecanoic acid, methyl ester	33.9
19	octadecanoic acid, methyl ester	35.8
20	eicosanoic acid, methyl ester	39.3

As previously discussed, no sulfur-containing compounds were identified in the pyrogram of the lignin sample, which further supports the origination of this element (quantified in the elemental analysis) from sulfuric acid that had not been completely eliminated at the end of the extraction step.

3.1.6 Field-emission scanning electron microscopy (FESEM)

FESEM images of the *E. grandis* lignin sample are shown in **Figure 4**. The surface of the material is highly irregular, with unevenness and undulations, which are consistent with the dehydration of vegetable tissues by drying processes [56,57]. In addition, the particles that compose the lignin sample are highly heterogeneous in terms of both shape and size, and they show high roughness. Similar morphologies were observed by Taleb et al. [53] for modified lignin from coffee grounds, by Bortoluz et al. [28] for lignin from *Pinus elliottii* sawdust and by Poletto et al. [58] for lignin from *E. grandis* sawdust. Finally, this analysis showed that *E. grandis* lignin has a favourable morphology for the removal of dyes, such as MB.

Figure 4. FESEM images of *E. grandis* lignin with magnification levels of **(a)** 500 × and **(b)** 2,000 ×

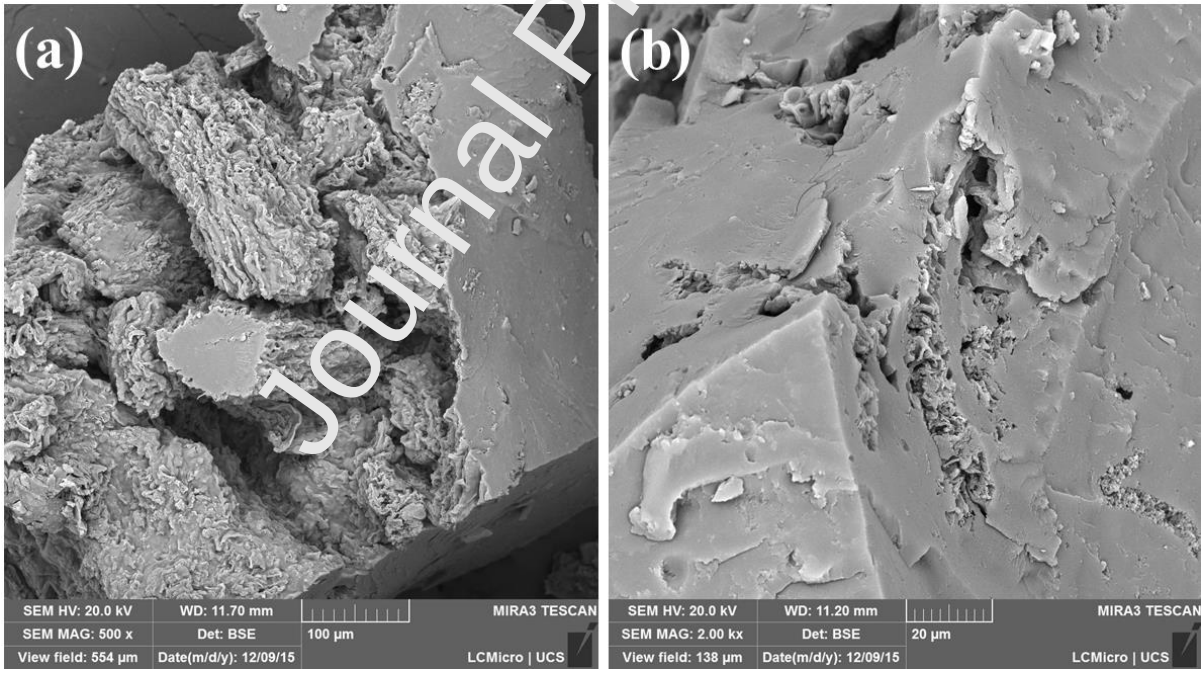

3.1.7 Thermogravimetric analysis (TG)

Figure 5 shows the thermogravimetric curve (TG) of the *E. grandis* lignin sample and its first derivative (DTG). The DTG curve shows that three main mass loss events occurred during the thermal degradation of the lignin: The first stage of decomposition occurs at approximately 70 °C and corresponds to the loss of sample moisture that was not

completely removed during the drying step that was carried out at the end of the extraction procedure. The second event, in which the highest rate of mass loss occurs (38.5%), was observed at 395 °C and, according to Beall and Eilckner [59], refers to the degradation of aliphatic side chains of the lignin structure. Similar results have been obtained by other authors, such as Pereira et al. [60], who evaluated the thermal decomposition of lignin samples extracted from *Eucalyptus* spp. Finally, the third and last event occurs gradually at a maximum temperature of approximately 630 °C; in this event, the mass loss is attributed to the depletion of aromatic rings from the chemical structure of lignin [22]. The knowledge of these properties enables the evaluation of the adsorption process at high temperatures since the material has satisfactory thermal stability.

Figure 5. TG and DTG curves of the *E. grandis* lignin

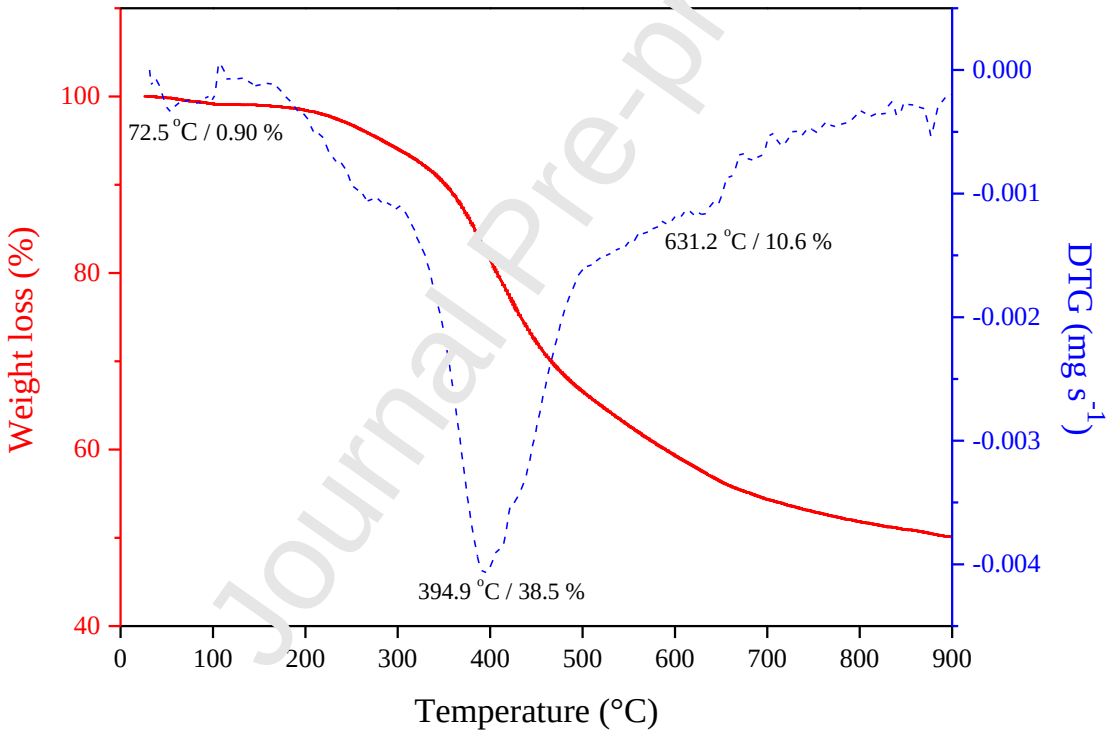

3.1.8 Specific surface area (BET) and pore size (BJH)

The obtained adsorption and desorption isotherms of N_2 for the *E. grandis* lignin sample are shown in **Figure 6**. These isotherms behave similarly to isotherms classified as type V, according to the International Union of Pure and Applied Chemistry (IUPAC) [61], which suggests the occurrence of adsorption in mesoporous materials through weak interactions. There is also a hysteresis loop, which indicates the possible presence of metastable fluid states within the pores, interconnected pores, or even pores without a defined structure [62].

Figure 6. N_2 adsorption and desorption isotherms for *E. grandis* lignin

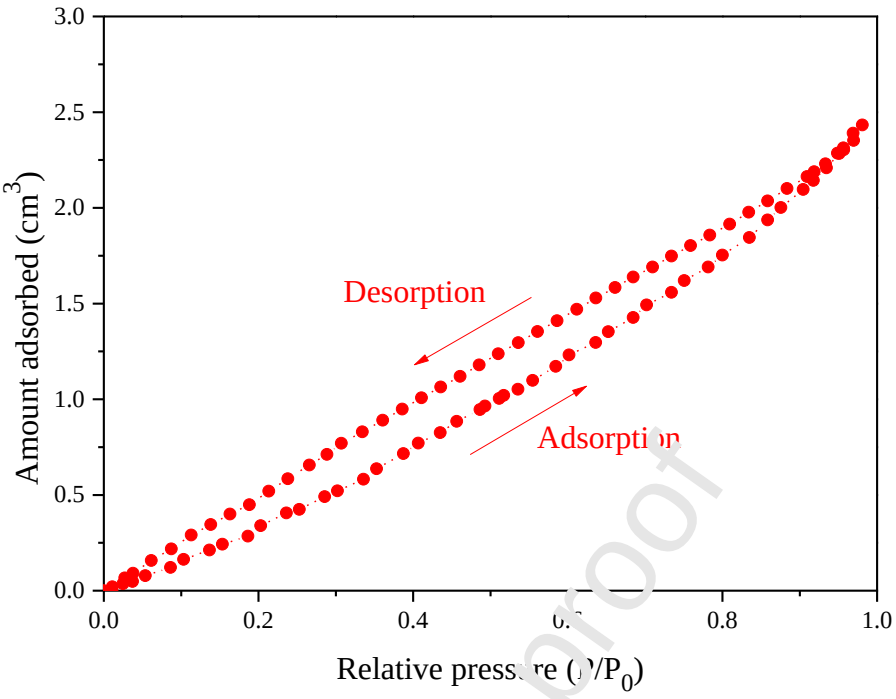

The presence of pores was demonstrated by the BJH method, which is usually applied to determine the radius and volume of pores in mesoporous materials. The lignin sample has an irregular pore distribution profile, which is in accordance with the hysteresis loop in **Figure 6**. Moreover, the material is mostly mesoporous, with a maximum pore value of approximately 25 Å; thus, the material is heterogeneous, as previously determined in the FESEM analysis (**Figure 4**). These results demonstrate that the lignin of *E. grandis* has pores of adequate size for the adsorption of the MB, which has a molecular diameter of between 8 and 9 Å [63].

The specific surface area determined using the desorption isotherm and the BET method was approximately 20 $m^2\ g^{-1}$. This value is relatively small when compared to that of activated carbon fibres obtained from lignin [64] but relatively large when compared to that for straw lignin [65], as presented in **Table 5**. The small values found for the surface area, volume and pore radius are likely due to the sample preparation procedures, mainly the drying method and conditions [65].

Table 5. Specific surface areas of various lignin samples

Residue	**Specific area ($m^2\ g^{-1}$)**	**Reference**
Straw lignin	0.1	[53]
E. grandis lignin	20	This work
Activated carbon fibres from lignin	3100	[52]

3.1.9 pH at the zero-charge point (pH_{PZC})

The results regarding the pH_{PZC} determination for the *E. grandis* lignin sample are presented in **Figure 7**. According to Raij [66], the pH_{PZC} is the pH value at which there is equality between the positive and negative charges on the surface of a material, and with this information, it is possible to describe the properties that result from the double electrical layer at the interface of a material under various pH conditions.

Figure 7. Determination of the pH_{PZC} of *E. grandis* lignin. Experimental conditions: pH = 2.0-11.0; lignin dosage = 100 mg; temperature = 25 °C; and contact time = 24 h

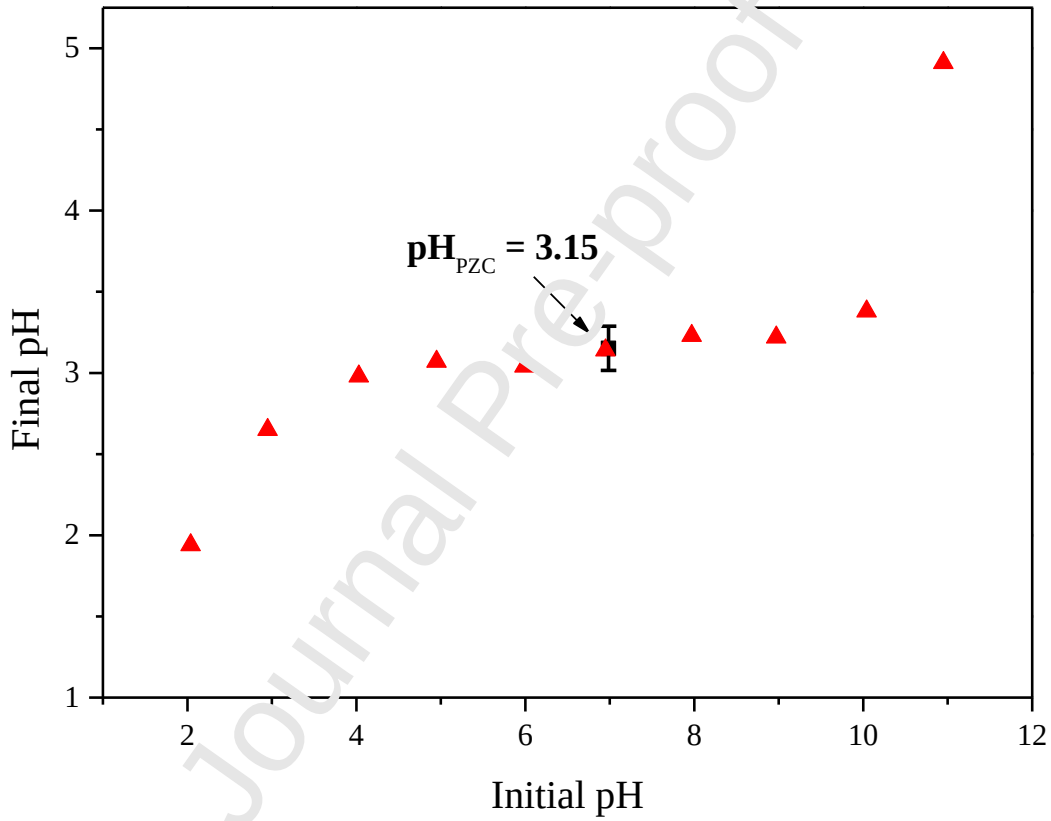

When the pH of the medium is lower than the pH_{PZC}, the adsorbent material is positively charged, which favours the adsorption of adsorbates with negative charge density, such as anionic dyes. If the pH of the medium exceeds the pH_{PZC}, the adsorbent is negatively charged, which favours the adsorption of adsorbates with positive charges, such as MB and other cationic dyes [67].

According to **Figure 7**, the pH_{PZC} value of the *E. grandis* lignin sample is equal to 3.15, from which we infer that the process of adsorption of MB by the lignin should be favoured in scenarios with pH > 3.15.

3.2 Adsorption experiments

3.2.1 Effect of the lignin dosage

Figure 8 presents the influence of the *E. grandis* lignin dosage on the MB removal performance. The results show that *%R* presents an increasing trend as the lignin dosage increases. This may be due to the availability of more active sites for adsorption [15]. In contrast, the q_t values exhibit the opposite trend. Hence, larger amounts of adsorbent promote greater MB removal but also reduce the yield, with smaller amounts of dye adsorbed per gram of lignin.

Figure 8. Influence of the *E. grandis* lignin dosage on the MB removal performance. Experimental conditions: pH = 5.6; stirring intensity = 150 rpm; temperature = 25 °C; contact time = 8 h; and MB concentration = 100 mg L^{-1}

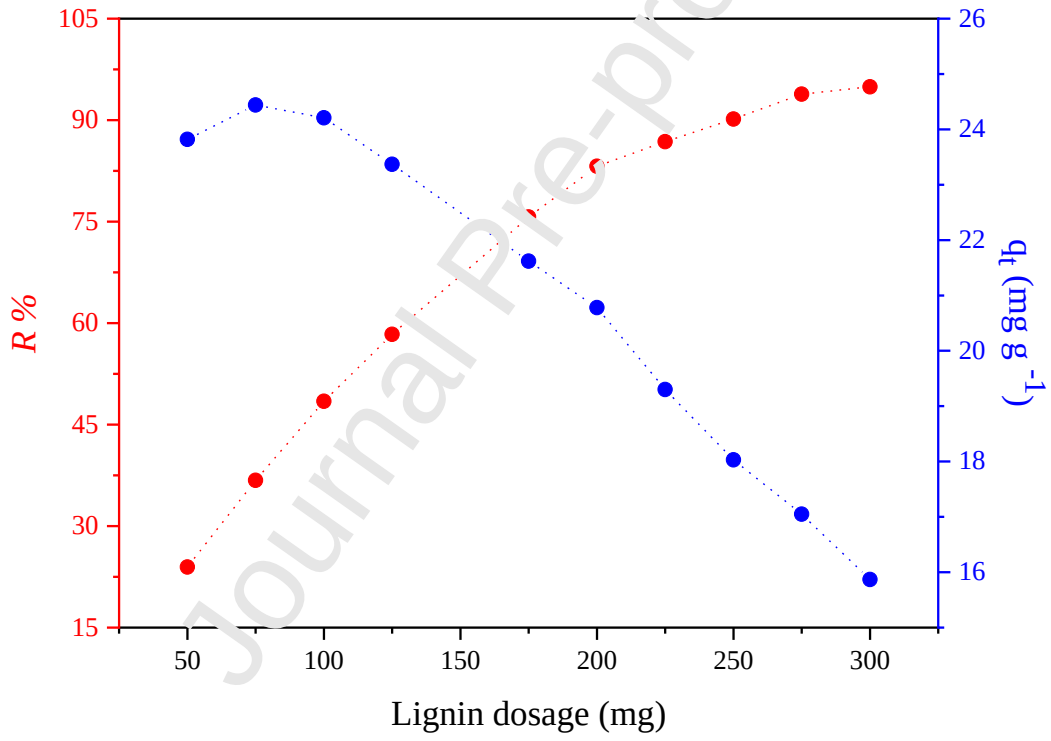

The lignin dosage for the other adsorption tests was selected by considering amounts of adsorbent for which *%R* was at least 80%. A mass of 225 mg was selected since larger masses would generated more waste. In addition, the gains in terms of *%R* are not highly significant as it would be necessary to increase the amount of lignin by approximately 11% to realize an increase in *%R* of approximately 4%.

3.2.2 Effect of the stirring frequency

The results regarding the effect of the stirring frequency of the system on the MB removal performance by the *E. grandis* lignin sample are presented in **Figure 9.**

Figure 9. Effect of the stirring frequency on the MB removal performance. Experimental conditions: pH = 5.6; lignin dosage = 225 mg; temperature = 25 °C; contact time = 8 h; and MB concentration = 100 mg L^{-1}

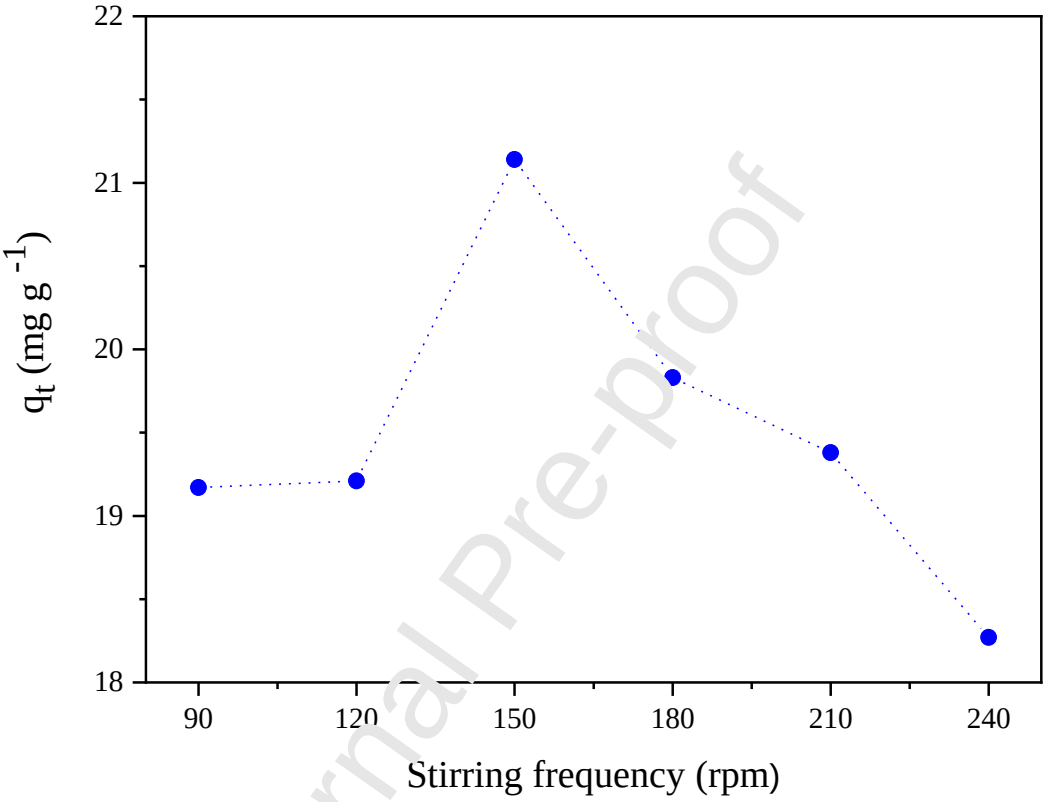

The value of q_t is maximal when the stirring frequency of the system is 150 rpm. For values that exceed 150 rpm, q_t tends to decrease slightly; hence, an increase in the stirring frequency in this range is unfavourable to the adsorbent-adsorbate interaction since the high turbulence rate of the medium promotes the dragging of the molecules of MB by the fluid before they can interact with the lignin [68]. Therefore, the stirring frequency was fixed to 150 rpm to carry out the other adsorption tests.

3.2.3 Effect of the pH

Figure 10 shows the influence of pH on the MB removal performance by the *E. grandis* lignin sample. According to this plot, q_t reaches its minimum values under highly acidic (pH < 4.0) or highly alkaline (pH > 9.0) conditions. In these two scenarios, a weak

interaction likely occurs between the MB and lignin due to the excess H_3O^+ and OH^- ions present in the medium and the competition between these species [69].

Figure 10. Effect of the initial pH on the MB removal performance. Experimental conditions: stirring frequency = 150 rpm; lignin dosage = 225 mg; temperature = 25 °C; contact time = 8 h; and MB concentration = 100 mg L^{-1}

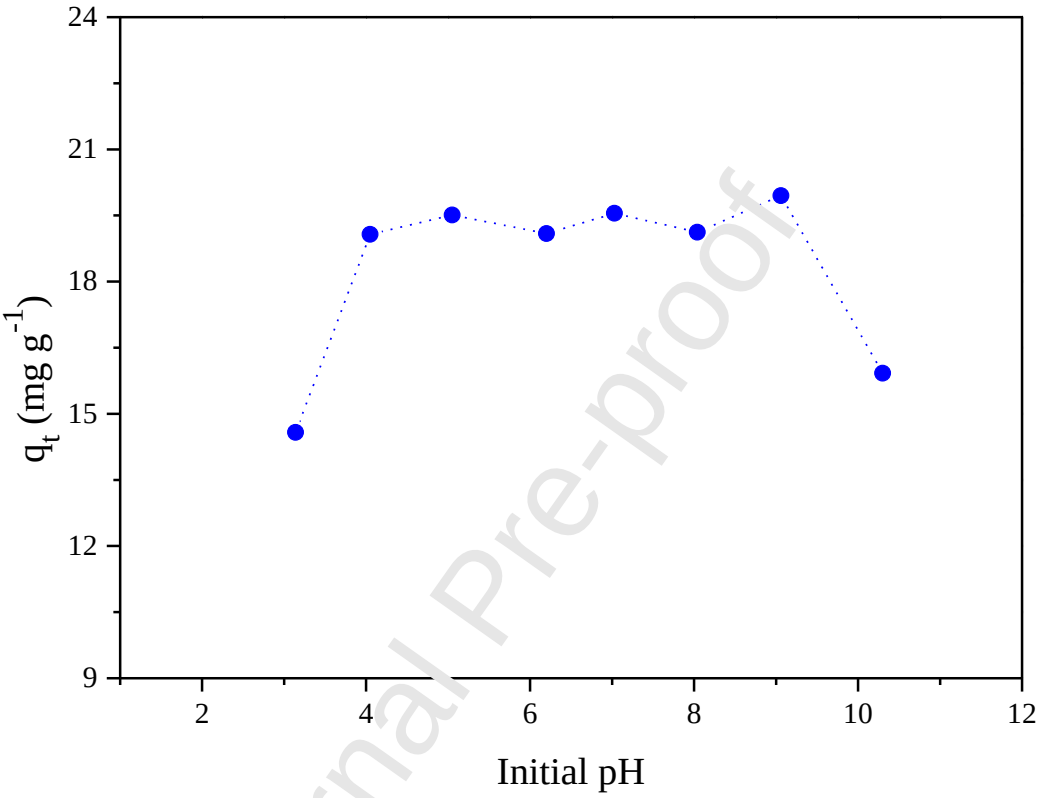

This behaviour is supported by the pH_{PZC} value of the adsorbent, namely, 3.15. At pH values for which pH < pH_{PZC}, the lignin is positively charged, namely, it has the same charge as the MB, thereby resulting in electrostatic repulsion between them. In contrast, at values of pH > pH_{PZC}, the lignin is negatively charged, which should, in principle, favour the interaction with the adsorbate, thereby implying an increase in the q_t values since MB is a cationic dye. However, at pH = 5.0, the values of q_t remain practically constant (with an average value of q_t = 19.5 mg g^{-1}) until pH = 9.0.

In practice, MB at pH > 5.6 is of the leuco-MB form (**Figure 11**) [70]. Under this condition, no relocated is relocated on the dye structure, and the electrostatic interactions between the adsorbent (which is negatively charged) and the adsorbate are disadvantaged. Therefore, in this region of pH values, the mechanism of interaction between the adsorbent and the adsorbate is likely to be mediated by π-π interactions that occur between the aromatic system of the dye and the aromatic portions of the chemical structure of lignin [71].

Figure 11. Chemical structure of MB as a function of the pH

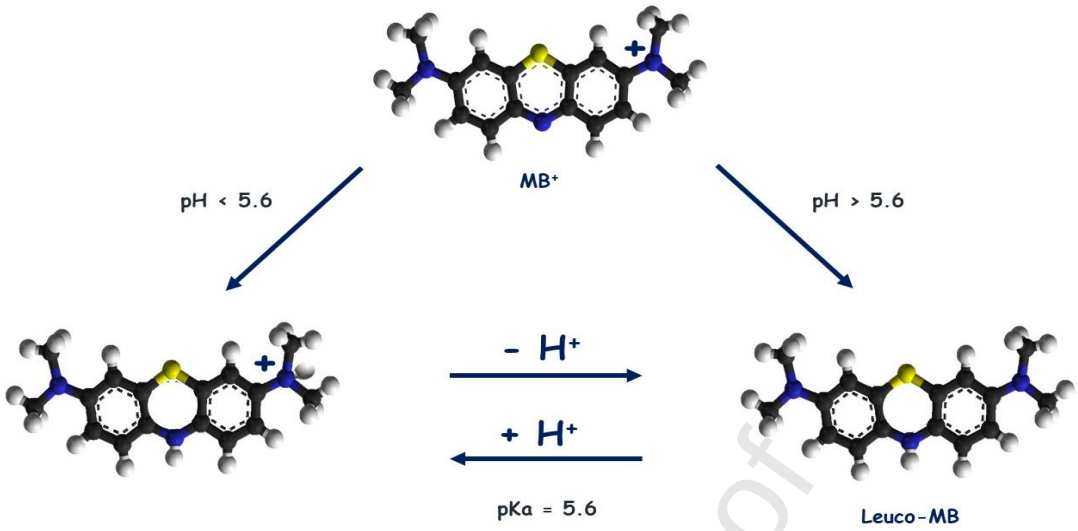

Based on these observations, the optimal pH values for carrying out the adsorption tests as a function of the initial pH are in the range of 5.0 to 8.0, where the best gains in terms of q_t occur. In this context, a pH value of 5.6 was selected for the other adsorption tests since the difference in terms of *%R* is less than 3% compared to the result obtained at pH = 9.0.

3.2.4 Effect of initial dye concentration and contact time

The adsorption tests that were carried out to evaluate the influence of the initial dye concentration showed that the increase in the MB concentration leads to an increased adsorption capacity of the *E. grandis* lignin. This behavior may be associated with the fact that more concentrated MB dye solutions provide a larger amount of adsorbate particles near the adsorbent surface and, consequently, a lower resistance to MB mass transfer between the aqueous and solid phases [72].

Moreover, the data set revealed that the MB dye removal occurs rapidly within the first 50 min of contact time and then proceeds gradually until 6 h. From this point, the q_t values differ by less than 1% from the final value obtained after 8 h, showing that the equilibrium has been reached. For this reason, the contact time selected for our study was fixed at 8 h.

Zhang et al. [25] observed analogous behavior for the adsorption of MB dye by lignin from rice straw. In this case, the adsorption process is favored in the first 30 min since at this stage, there is a greater quantity of active sites available on the adsorbent surface. After a certain period of time, many of these sites are already occupied, and consequently, the interaction with the remaining sites is difficult due to the repulsion between the adsorbed and nonadsorbed dye molecules (steric impediment).

Finally, this study also shows that the MB concentration of 100 mg L^{-1} is the most appropriate for evaluation of the thermodynamics in the present study. Higher MB concentrations require high dilution factors to determine the final concentration of the MB solution by visible spectrophotometry, which increases the chances of very large reading errors. Moreover, 100 mg L^{-1} is an intermediate concentration in real wastewater from the textile industry, as dye concentrations generally range from 10 to 200 mg L^{-1}, depending on the fiber and dye type used [73].

3.2.5 Equilibrium studies

Table 6 presents the parameters identified for the Freundlich, Langmuir, Temkin and Dubinin-Radushkevich models, while **Figure 12** shows the isotherms in their nonlinear forms. To determine whether these models differ statistically, Fisher's test was conducted by evaluating the isotherms in pairs.

Table 6. Parameters obtained from the Freundlich, Langmuir, Temkin and Dubinin-Radushkevich isotherm models and the *Fisher* test

Isotherm model	Parameter	Obtained value
Freundlich	k_F (mg g^{-1} (L $mg^{-1})^{1/n}$)	2.12
	1/n	0.524
	R^2	0.9475
	F_{obj}	0.785
Langmuir	k_L (L mg^{-1})	0.0223
	R_L	0.473 – 0.230
	q_m (mg g^{-1})	31.97
	R^2	0.9540
	F_{obj}	0.762
Temkin	A_t (L g^{-1})	0.229
	b_t (J mg^{-1})	6.81
	R^2	0.9441
	F_{obj}	0.833
Dubinin-Radushkevich	q_s (mg g^{-1})	23.1
	k_{ad} (mol^2 J^{-2})	0.00661
	R^2	0.9204
	F_{obj}	1.20
Fisher test		
F_{min} = 0.0648	F_{max} = 15.4	
Comparison between isotherm models	***F value***	
Freundlich vs. Langmuir	1.03	
Freundlich vs. Temkin	0.941	
Freundlich vs. Dubinin-Radushkevich	0.649	
Langmuir vs. Temkin	0.914	
Langmuir vs. Dubinin-Radushkevich	0.630	
Temkin vs. Dubinin-Radushkevich	0.689	

The results demonstrate that for all of the evaluated pairs, the F value is within the F_{min} and F_{max} intervals. Thus, all of the tested isothermal models can be considered identical to one another (based on a 95% confidence interval). This result can also be observed in **Figure 12**, where all models show a satisfactory adjustment to the experimental data. Among these values, the Freundlich *vs*. Langmuir pair resulted in an F value more distant from the F_{min} and F_{max} extremes; hence, these models are the most compatible with each other, and both can describe the adsorption process. However, to better understand the adsorption process, is necessary to also consider the values of R^2 and F_{obj}.

Figure 12. Experimental data adjusted to the Freundlich, Langmuir, Temkin and Dubinin-Radushkevich isotherms

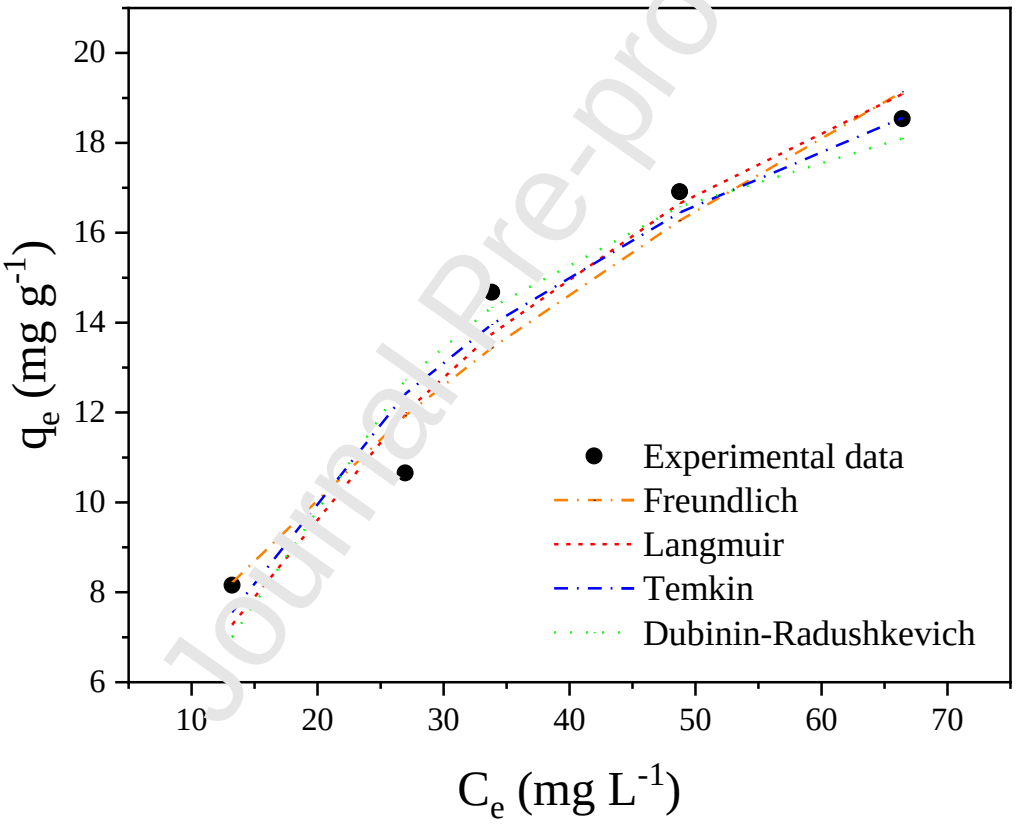

According to the analysis of the F_{obj} values, the error associated with the experimental data is smaller for the Langmuir model. In addition, the value of R^2 indicates that there is a better correlation of data for this model. Thus, regardless of whether other models also provide information on the analysed adsorption process, the Langmuir model is even more suitable for this objective. In the study of Taleb et al. [53], it was also found that Langmuir is the most suitable model for describing the adsorption of MB by lignin from coffee grounds. This result demonstrates that the adsorption process of the MB by *E. grandis* lignin occurs in

a homogeneous system without interaction between the adsorbed molecules and that there is monolayer coverage [27,74].

Comparing the q_m value of the *E. grandis* lignin with those of other similar materials that have also been used to remove MB, the *E. grandis* lignin had a relatively low maximum adsorption capacity compared to modified lignins, such as sulfonate lignin-based hydrogels [26] and lignin-based activated carbon from black liquor [75]. However, compared to lignins used in native form, it presented a similar result [25,53]. **Table 7** presents additional details on the results obtained in these studies.

Table 7. Comparison with modified and native lignins in terms of the q_m values and operational conditions for MB adsorption

Adsorbent	q_m (mg g^{-1})	Operational conditions	Reference
Sulfonate lignin-based hydrogels	540.5	Adsorbent dosage = 40 mg; Temperature = 30 °C; Contact time = 24 h; MB concentration = 100 to 1,000 mg L^{-1}	[26]
Lignin-based activated carbon from black liquor	92.51	Stirring frequency = 200 rpm; Adsorbent dosage = 50 mg; Temperature = 25 °C; pH = 5.0 – 6.0; Contact time = 16 h; MB concentration = 100 to 400 mg L^{-1}	[75]
E. grandis lignin	31.97	Stirring frequency = 150 rpm; Adsorbent dosage = 225 mg; Temperature = 25 °C; pH = natural; Contact time = 8 h; MB concentration = 50 to 150 mg L^{-1}	This study
Lignin from rice straw	40.02	Adsorbent dosage = 100 mg; Temperature = 20 °C; Contact time = 24 h; MB concentration = 10 to 200 mg L^{-1}	[25]
Lignin from coffee grounds	66.22	Adsorbent dosage = 60 mg; Temperature = 25 °C; pH = natural; Contact time = 24 h; MB concentration = 10 to 100 mg L^{-1}	[53]

Although the q_m value of *E. grandis* lignin is significantly lower than those of modified lignins, this adsorbent does not require high temperatures during its processing or activation steps; hence, it has a lower production cost. Regarding the constant k_L, the value reported here is lower than that obtained by Zhang et al. [25] (0.2083 L mg^{-1}), who evaluated the adsorption of MB by lignin from rice straw, but close to that obtained by Zou et al. [74] (0.0750 L mg^{-1}), who analysed MB removal using modified pine sawdust. The values for the parameter R_L are equal to 0.473 (at the lowest concentration of MB) and 0.230 (at the highest concentration of MB) and are within the range of $0 < R_L < 1$, which demonstrates once again that the process of adsorption of MB by *E. grandis* lignin is favourable [32].

3.2.6 Kinetic studies

Table 8 presents the parameters identified for the pseudo-first-order and pseudo-second-order kinetic models. The results of the *F* test demonstrate that, in a first analysis, the evaluated kinetic models are statistically identical within the range of MB concentrations when using a 95% confidence level. However, for all cases, the pseudo-second-order model showed the best correlation (R^2) with the experimental data. Additionally, the results obtained for F_{obj} in the pseudo-second-order model show that the errors associated with the experimental data are smaller than those of the pseudo-first-order model. Thus, the pseudo-second-order model was regarded the most suitable for assessing the MB removal rate by the lignin sample.

According to Yagub et al. [10], most studies on the adsorption of dyes by lignocellulosic materials show that the best adjustments are obtained primarily with the pseudo-second-order model. In this context, examples are presented in the studies of Zhang et al. [25] and Ponnusami et al. [76], which evaluated MB removal by lignin from rice husk and from guava leaf, respectively.

The largest value of the kinetic constant of the pseudo-second-order (k_2) model was identified for the concentration of 100 mg L^{-1}; thus, under this experimental condition, the process reaches equilibrium faster than with other concentrations of MB. According to the literature, the value of k_2 depends strongly on the initial concentration of dye in the medium, and higher removal rates are often associated with lower concentrations. However, Plazinski et al. [77] explain that although this behaviour is commonly observed, this parameter will not always depend directly on the experimental conditions of the process. Doğan et al. [78], for example, evaluated MB removal by perlite and observed a behaviour similar to that reported by this study. The adsorption of this dye was conducted in batches using solutions with

concentrations that ranged from 50 to 80 mg L^{-1}, and the largest k_2 value (0.0861 g mg^{-1} min^{-1}) was observed for the solution with a concentration of 65 mg L^{-1}.

Table 8. Kinetic parameters for the nonlinear pseudo-first- and pseudo-second-order models

Parameter	MB dye concentrations (mg L^{-1})				
	50	**75**	**100**	**125**	**150**
Pseudo-first order					
$q_{t\,(exp)}$ (mg g^{-1})	8.15	12.47	15.68	18.75	22.10
$q_{t\,(cal)}$ (mg g^{-1})	6.76	10.15	14.81	16.29	18.05
$k_1 \times 10^{-3}$ (min^{-1})	0.0451	0.301	0.482	0.513	0.241
R^2	0.8947	0.8749	0.9942	0.8950	0.9141
F_{obj}	0.753	1.58	0.137	3.35	3.355
Pseudo-second order					
$q_{t\,(exp)}$ (mg g^{-1})	8.15	12.47	15.68	18.75	22.10
$q_{t\,(cal)}$ (mg g^{-1})	7.62	10.58	14.94	16.59	18.58
$k_2 \times 10^{-3}$ (g mg^{-1} min^{-1})	0.00640	0.0404	0.118	0.0766	0.0234
R^2	0.9433	0.9094	0.9957	0.9041	0.9183
F_{obj}	0.405	1.15	0.102	3.06	3.19
Fisher test					
F_{min}			0.172		
F	1.86	1.38	1.34	1.09	1.05
$F_{máx}$			5.82		

3.2.7 Thermodynamic parameters

The results regarding the thermodynamic parameters for MB removal by the *E. grandis* lignin are presented in **Table 9**. According to these results, the value of $\Delta G°_{ads}$ decreases as the temperature increases; hence, the spontaneity of the adsorption increases. This behaviour is characteristic of endothermic processes in which an increase in temperature

favours dye removal. Similar results were also reported by Akkaya and Güzel [79] and Zou et al. [74], who evaluated MB removal by cucumber peels and by *Pinus tabulaeformis* sawdust, respectively.

Table 9. Thermodynamic parameters for MB removal

T(K)	k_c	$\Delta G°_{ads}$ (kJ mol^{-1})	$\Delta H°_{ads}$ (kJ mol^{-1})	$\Delta S°_{ads}$ (J mol^{-1}K^{-1})	R^2
278	1.31	– 0.620			
288	2.44	– 2.14			
298	3.74	– 3.27	+38.64	+141.3	0.9971
308	6.86	– 4.93			
318	10.82	– 6.30			

The obtained $\Delta H°_{ads}$ value exceeds zero, thereby proving that the adsorption process is endothermic, which is supported by the other results and discussed in the present study. Its magnitude is within the range for physical adsorption; hence, the interactions between the MB molecules and the *E. grandis* lignin are of this type [79,80]. If the regression of experimental equilibrium data follows the Langmuir model, chemical adsorption typically occurs. However, Dąbrowski [81] explains that the Langmuir model can also describe physical adsorption satisfactorily.

Finally, the positive value found for $\Delta S°_{ads}$ indicates that there is an increase in the randomness of the system. Thus, the disorder at the solid-solution interface increases occurs during adsorption [82].

3.3 Suggested mechanism for MB removal by *E. grandis* lignin

Based on the results obtained in this work, it was possible to outline the main mechanisms responsible for the adsorption of the MB molecules by the *E. grandis* lignin sample. **Figure 13** illustrates these possible interactions. According to the FT-IR and ^{13}C NMR spectroscopy analyses, *E. grandis* lignin has a structure rich in oxygenated functional groups. These functional groups can interact with MB molecules through hydrogen bonds, which are one of the main intermolecular forces responsible for adsorption. In addition, the incidence of aromatic rings in the chemical structure of the lignin and in the structure of the dye can also favour π- π interactions, thereby contributing to the MB removal by the lignin [83,84].

Figure 13. Possible interactions between the MB molecules and *E. grandis* lignin

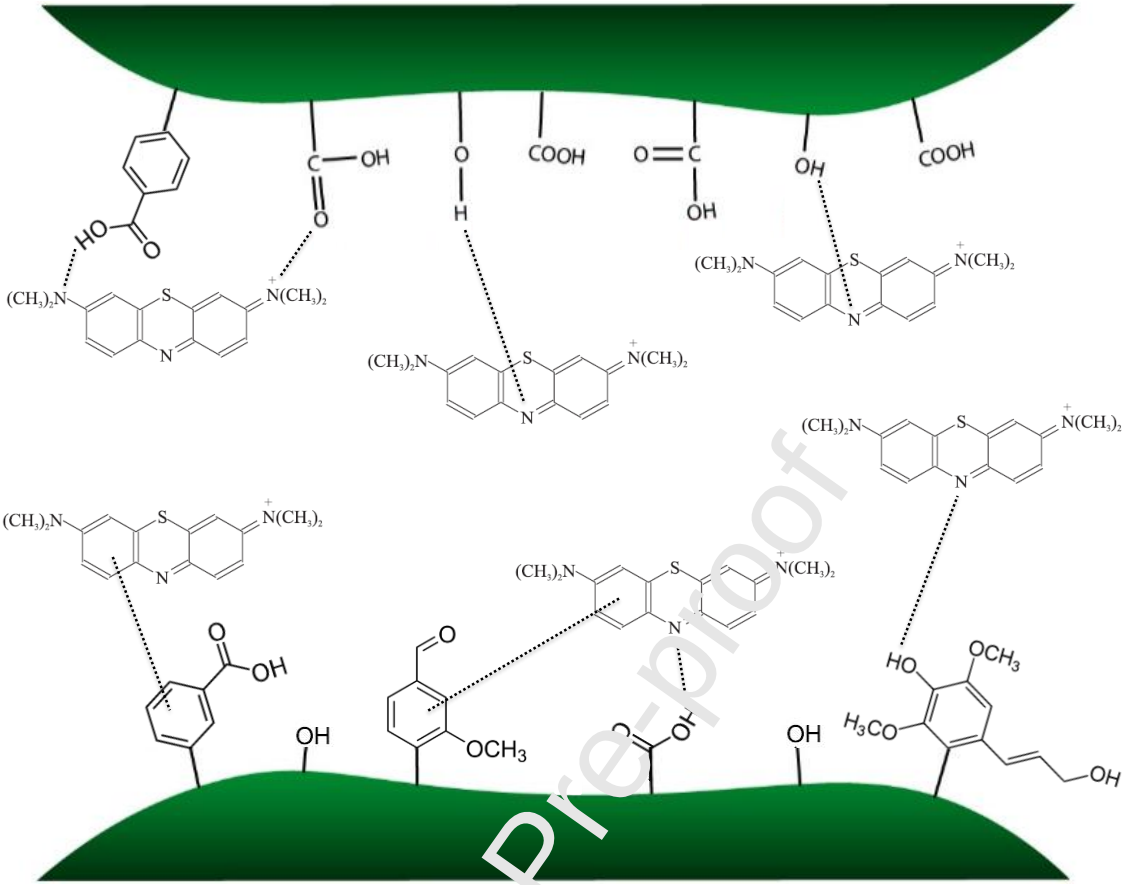

Finally, it was determined that electrostatic interactions had little or no influence on the adsorption of MB by the *E. grandis* lignin. According to the experiment in which the effect of the initial pH of the medium was examined, the superficial charges of the adsorbent and the adsorbate are not opposed when the pH exceeds the pH_{PZC} due to the leuco form of the MB dye at pH > 5.6.

3.4 Regeneration of the *E. grandis* lignin

After MB removal by the *E. grandis* lignin sample from aqueous solutions, the dye was desorbed from the adsorbent with Milli-Q water to investigate the possibility of reusing the adsorbent in other removal cycles. **Figure 14** summarizes these results.

The obtained values for *%R* decrease as the lignin is reused, with a larger decrease from the first to the second use (~ 13.5%), which was followed by a smaller decrease in the next step (~ 2.9%), and an even smaller decrease from the third to the fourth use (~ 2.8%). The difference between the first and the fourth uses is approximately 19%; hence, the *E. grandis* lignin can be regenerated at least four times to remove MB without a significant loss of efficiency.

Figure 14. Reuse of the *E. grandis* lignin. Experimental conditions: C_0 = 100 mg L^{-1}; m = 225 mg; v = 150 rpm; t = 8 h; and T = 25 °C

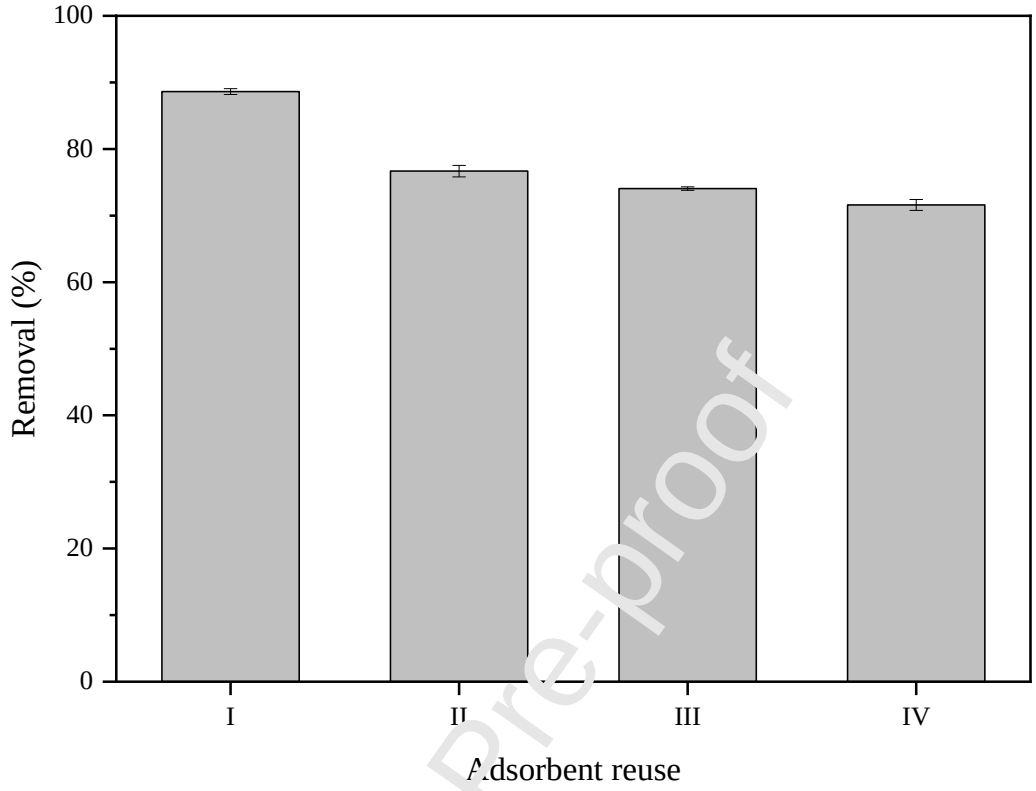

These results demonstrate that even after the two stages of desorption, MB molecules remain bound to the lignin due to a phenomenon that has been referred to as "irreversible adsorption" [85,86]. This can be observed in **Figure 15,** which shows lignin with a greenish colour after the end of the first desorption process, which differs substantially from its crude form (before the first adsorption test).

Figure 15. *E. grandis* lignin appearance: **(a)** before and **(b)** after the first desorption

4. Conclusions

This study reports the extraction of *E. grandis* lignin and its use in MB removal from aqueous solutions by adsorption. The method proved to be suitable for the extraction of the lignin from a sawdust sample since it was demonstrated through characterization analyses that the obtained material has characteristics similar to those reported in the literature. The characterization data showed the presence of several functional groups, among them phenolic hydroxyl and methoxyl groups, along with both surface and morphological heterogeneity. The specific surface area of the *E. grandis* lignin was determined to be 20 m^2 g^{-1}. Regarding pH_{PZC}, it was found that the pH required to neutralize the material surface was equal to 3.15 and that this characteristic influences the sample's adsorption capacity.

Regarding the optimization of the adsorption process variables, it was found that all of the variables influence the removal of MB by the lignin sample. The values obtained in this optimization for the contact time (8 h), adsorbent dosage (225 mg), stirring frequency (150 rpm), and initial pH (5.6) proved to be the most suitable for the process overall, and removal rates of approximately 90% were realized.

According to the adsorption equilibrium studies, the Langmuir model was the model that best fit the experimental data; hence, the interaction between MB and *E. grandis* lignin is favourable and occurs with the formation of monolayers. The values obtained for the Langmuir isothermal constant (k_l) and maximum adsorption capacity (q_m) were 0.0223 L mg^{-1} and 31.97 mg g^{-1}, respectively. Regarding the kinetics, the pseudo-second-order model best represented the obtained experimental data. The values obtained for the kinetic constant (k_2) varied between 0.00640 and 0.118 g mg^{-1} min^{-1}; thus, the process is slow and, therefore, equilibrium is not reached quickly under the investigated experimental conditions. According to the thermodynamic parameters, the process is spontaneous ($\Delta G°_{ads} < 0$), and there is an affinity between the adsorbent and adsorbate. In addition, the value of $\Delta S°_{ads}$ (+141.3 J mol^{-1} K^{-1}) showed that there is an increase in the system randomness, while the value of $\Delta H°_{ads}$ (+38.64 kJ mol^{-1}) showed that the adsorption is endothermic and physical.

Finally, the use of waste from the furniture industry and, more specifically, from lignins from these materials, is a viable alternative for the removal of dyes from water. In addition, it is concluded that its use as an adsorbent contributes to the minimization of the impacts of its inappropriate disposal into the environment.

5. Acknowledgements

The authors would like to thank Coordenação de Aperfeiçoamento de Pessoal de Nível Superior (CAPES - Finance Code 001), Conselho Nacional de Desenvolvimento Científico e Tecnológico (CNPq), CESAM (UID/AMB/50017/2019), and FCT/MEC for their financial support.

The NMR spectrometer is part of the National NMR Network (PTNMR) and is partially supported by Infrastructure Project Nº 022161 (co-financed by FEDER through COMPETE 2020, POCI and PORL and FCT through PIDDAC).

6. References

[1] C. Jiang, X. Wang, D. Qin, W. Da, B. Hou, C. Hao, Construction of magnetic lignin-based adsorbent and its adsorption properties for dyes, J. Hazard. Mater. 369 (2019) 50–61. https://doi.org/10.1016/j.jhazmat.2019.02.021

[2] N.B. Singh, G. Nagpal, S. Agrawal, Rachna, Water purification by using adsorbents: a review, Environ. Technol. Innov. 11 (2018) 187–240. https://doi.org/10.1016/j.eti.2018.05.006

[3] G. Varadarajan, P. Venkatachalam, Sustainable textile dyeing processes, Environ. Chem. Lett. 14 (2016) 113–122. https://doi.org/10.1007/s10311-015-0533-3

[4] C.R. Holkar, A.J. Jadhav, D. V Pinjari, N.M. Mahamuni, A.B. Pandit, A critical review on textile wastewater treatments: possible approaches, J. Environ. Manage. 182 (2016) 351–366. https://doi.org/10.1016/j.jenvman.2016.07.090

[5] R. Kant, Textile dyeing industry an environmental hazard, Nat. Sci. 4 (2012) 22–26. https://doi.org/http://dx.doi.org/10.4236/ns.2012.41004

[6] H. Singh, R. Singh, V. Kaur, Prospects of silatranyl dye derivatives in cotton dyeing process and dye effluent treatment: a comparative study of methyl red and its silatranyl derivative, Cellulose 26 (2019) 2885–2894. https://doi.org/10.1007/s10570-019-02293-4

[7] N. Supanchaiyamat, K. Jetsrisuparb, J.T.N. Knijnenburg, D.C.W. Tsang, A.J. Hunt, Lignin materials for adsorption: Current trend, perspectives and opportunities, Bioresour. Technol. 272 (2019) 570–581. https://doi.org/10.1016/j.biortech.2018.09.139

[8] C. Zaharia, D. Suteu, A. Muresan, A. Popescu, Textile wastewater treatment by

homogenous oxidation with hydrogen peroxide, Environ. Eng. Manag. J. 8 (2009) 1359–1369. https://doi.org/10.30638/eemj.2009.199

[9] C.C.I. Guaratini, M.V.B. Zanoni, Corantes têxteis, Quim. Nova. 23 (2000) 71–78. https://doi.org/10.1590/S0100-40422000000100013

[10] M.T. Yagub, T.K. Sen, S. Afroze, H.M. Ang, Dye and its removal from aqueous solution by adsorption: A review, Adv. Colloid Interface Sci. 209 (2014) 172–184. https://doi.org/10.1016/j.cis.2014.04.002

[11] S. Lalnunhlimi, V. Krishnaswamy, Decolorization of azo dyes (Direct Blue 151 and Direct Red 31) by moderately alkaliphilic bacterial consortium, Brazilian J. Microbiol. 47 (2015) 39–46. https://doi.org/10.1016/j.bjm.2015.11.013

[12] A. Bhatnagar, M. Sillanpää, Utilization of agro-industrial and municipal waste materials as potential adsorbents for water treatment - a review, Chem. Eng. J. 157 (2010) 277–296. https://doi.org/10.1016/j.cej.2010.01.007

[13] L. Zhang, W. Xue, L. Gu, Modification of hyperbranched hemicellulose polymer and its application in adsorbing acid dyes, Cellulose 26 (2019) 5583–5601. https://doi.org/10.1007/s10570-019-02483-0.

[14] M. Rafatullah, O. Sulaiman, R. Hashim, A. Ahmad, Adsorption of methylene blue on low-cost adsorbents: a review, J. Hazard. Mater. 177 (2010) 70–80. https://doi.org/10.1016/j.jhazmat.2009.12.047

[15] Y. Jin, C. Zeng, Q.-F. Lü, Y. Yu, Efficient adsorption of methylene blue and lead ions in aqueous solutions by 5-sulfosalicylic acid modified lignin, Int. J. Biol. Macromol. 123 (2019) 50–58. https://doi.org/https://doi.org/10.1016/j.ijbiomac.2018.10.213

[16] L.R. Bonetto, J.S. Crespo, R. Guégan, V.I. Esteves, M. Giovanela, Removal of methylene blue from aqueous solutions using a solid residue of the apple juice industry: full factorial design, equilibrium, thermodynamics and kinetics aspects, J. Mol. Struct. 1224 (2021) 129296. https://doi.org/10.1016/j.molstruc.2020.129296

[17] L. Gelain, M. Antunes, J.S. Crespo, M. Giovanela, Removal of zinc(II) from aqueous solutions using an eco-friendly biosorbent originating from the winery industry, Sep. Sci. Technol. 49 (2014) 2212–2220. https://doi.org/10.1080/01496395.2014.913626

[18] M. Antunes, V.I. Esteves, R. Guégan, J.S. Crespo, A.N. Fernandes, M. Giovanela, Removal of diclofenac sodium from aqueous solution by Isabel grape bagasse, Chem. Eng. J. 192 (2012) 114–121. https://doi.org/10.1016/j.cej.2012.03.062

[19] O. Gordobil, R. Moriana, L. Zhang, J. Labidi, O. Sevastyanova, Assesment of technical lignins for uses in biofuels and biomaterials: structure-related properties, proximate

analysis and chemical modification, Ind. Crops Prod. 83 (2016) 155–165. https://doi.org/10.1016/j.indcrop.2015.12.048

[20] D. Pilo-Veloso, E.A. do Nascimento, A.L. de Morais, Isolamento e análise estrutural de ligninas, Quim. Nova. 16 (1993) 435–448.

[21] S. Huang, L. Wu, T. Li, D. Xu, X. Lin, C. Wu, Facile preparation of biomass lignin-based hydroxyethyl cellulose super-absorbent hydrogel for dye pollutant removal, Int. J. Biol. Macromol. 137 (2019) 939–947. https://doi.org/https://doi.org/10.1016/j.ijbiomac.2019.06.234

[22] D. Watkins, M. Nuruddin, M. Hosur, A. Tcherbi-Narteh, S. Jeelani, Extraction and characterization of lignin from different biomass resources, J. Mater. Res. Technol. 4 (2015) 26–32. https://doi.org/https://doi.org/10.1016/j.jmrt.2014.10.009

[23] D.R. Naron, F.X. Collard, L. Tyhoda, J.F. Görgens, Characterisation of lignins from different sources by appropriate analytical methods: introducing thermogravimetric analysis-thermal desorption-gas chromatography–mass spectroscopy, Ind. Crops Prod. 101 (2017) 61–74. https://doi.org/10.1016/j.indcrop.2017.02.041

[24] D. Suteu, T. Malutan, D. Bilba, Removal of reactive dye Brilliant Red HE-3B from aqueous solutions by industrial lignin: equilibrium and kinetics modeling, Desalination 255 (2010) 84–90. https://doi.org/10.1016/j.desal.2010.01.010

[25] S. Zhang, Z. Wang, Y. Zhang, H. Pan, L. Tao, Adsorption of methylene blue on organosolv lignin from rice straw, Procedia Environ. Sci. 31 (2016) 3–11. https://doi.org/10.1016/j.proenv.2016.02.001

[26] J. Li, H. Li, Z. Yuan, J. Fang, L. Chang, H. Zhang, C. Li, Role of sulfonation in lignin-based material for adsorption removal of cationic dyes, Int. J. Biol. Macromol. 135 (2019) 1171–1181. https://doi.org/10.1016/j.ijbiomac.2019.06.024

[27] R. Zhang, Y. Zhou, X. Gu, J. Lu, Competitive Adsorption of methylene blue and Cu^{2+} onto citric acid modified pine sawdust, CLEAN - Soil, Air, Water. 43 (2015) 96–103. https://doi.org/10.1002/clen.201300818

[28] J. Bortoluz, A. Cemin, L.R. Bonetto, F. Ferrarini, V.I. Esteves, M. Giovanela, Isolation, characterization and valorization of lignin from Pinus elliottii sawdust as a low-cost biosorbent for zinc removal, Cellulose 26 (2019) 4895–4908. https://doi.org/10.1007/s10570-019-02399-9

[29] Brazilian Tree Industry, Report 2019, 2019. https://iba.org/site/en/

[30] M. Poletto, A.J. Zattera, M.M.C. Forte, R.M.C. Santana, Thermal decomposition of wood: influence of wood components and cellulose crystallite size, Bioresour. Technol.

109 (2012) 148–153. https://doi.org/10.1016/j.biortech.2011.11.122

[31] I.D. Smičiklas, S.K. Milonjić, P. Pfendt, S. Raičević, The point of zero charge and sorption of cadmium (II) and strontium (II) ions on synthetic hydroxyapatite, Sep. Purif. Technol. 18 (2000) 185–194. https://doi.org/10.1016/S1383-5866(99)00066-0

[32] K.Y. Foo, B.H. Hameed, Insights into the modeling of adsorption isotherm systems, Chem. Eng. J. 156 (2010) 2–10. https://doi.org/10.1016/j.cej.2009.09.013

[33] H.M.F. Freundlich, Over the adsorption in solution, J. Phys. Chem. 57 (1906) 385–471.

[34] I. Langmuir, The constitution and fundamental properties of solids and liquids, J. Am. Chem. Soc. 252 (1916). https://doi.org/https://doi.org/10.1021/ja02268a002

[35] S. Lagergren, About the theory of so-called adsorption of soluble substances, K. Sven. Vetenskapsakademiens Handl. 24 (1898) 1–39.

[36] G. Blanchard, M. Maunaye, G. Martin, Removal of heavy metals from waters by means of natural zeolites, Water Res. 18 (1984) 1501–1507. https://doi.org/https://doi.org/10.1016/0043-1354(84)90124-6

[37] S. Da Ros, M. Schwaab, J.C. Pinto, Parameter estimation and statistical methods, Elsevier, 2017. https://doi.org/10.1016/B978-0-12-409547-2.13918-6

[38] D. Montgomery, Design and Analysis of Experiments, 5th ed., John Wiley & Sons, New York, 2001.

[39] M.Z. Xiao, W.J. Chen, S. Hong, B. Pang, X.F. Cao, Y.Y. Wang, T.Q. Yuan, R.C. Sun, Structural characterization of lignin in heartwood, sapwood, and bark of eucalyptus, Int. J. Biol. Macromol. 138 (2019) 519–527. https://doi.org/10.1016/j.ijbiomac.2019.07.137.

[40] K.S. Salem, V. Naithani, H. Jameel, L. Lucia, L. Pal, Lignocellulosic fibers from renewable resources using green chemistry for a circular economy, Glob. Challenges 2000065 (2020) 1–10. https://doi.org/10.1002/gch2.202000065.

[41] J.O. Brito, L.E.G. Barrichelo, Correlações entre características físicas e químicas da madeira e a produção de carvão vegetal: I. densidade e teor de lignina da madeira de eucalipto, Ipef. 14 (1977) 9–20.

[42] P.F. Trugilho, M.L. Bianchi, S.C. Da Silva Rosado, J.T. Lima, Qualidade da madeira de clones de espécies e híbridos naturais de Eucalyptus, Sci. For. Sci. 73 (2007) 55–62.

[43] D. Morais, S. A. L., Nascimento, E. A., Piló-Veloso, Determinação do grau de condensação e do número de grupos metoxila por unidade monomérica de ligninas do E. grandis por espectroscopia FTIR, Quim. Nova. 17 (1994) 4–8.

[44] E.D.O.S. Saliba, N.M. Rodriguez, S.A.L. De Morais, D. Piló-Veloso, Ligninas:

métodos de obtenção e caracterização química, Ciência Rural. 31 (2001) 917–928. https://doi.org/10.1590/S0103-84782001000500031

[45] J. Lin, G. Zhao, Preparation and characterization of high surface area activated carbon fibers from lignin, Polymers (Basel). 8 (2016). https://doi.org/10.3390/polym8100369.

[46] A. Singh, K. Yadav, A.K. Sen, Sal (Shorea Robusta) Leaves lignin epoxidation and its use in epoxy based coatings, Am. J. Polym. Sci. 2 (2017) 1–18. https://doi.org/10.5923/j.ajps.20120201.03

[47] T. Ainane, F. Khammour, M. Talbi, M.H. Elkouali, A novel bio-adsorbent of mint waste for dyes remediation in aqueous environments: study and modeling of isotherms for removal of methylene blue, Orient. J. Chem. 30 (2014) 1183–1189. https://doi.org/http://dx.doi.org/10.13005/ojc/300332

[48] M.K. Uddin, A. Nasar, Walnut shell powder as a low-cost adsorbent for methylene blue dye: isotherm, kinetics, thermodynamic, desorption and response surface methodology examinations, Sci. Rep. 10 (2020) 1–13. https://doi.org/10.1038/s41598-020-64745-3

[49] V. Karthik, P.S. Kumar, K.H. Vardhan, K. Saravanan, Adsorptive behaviour of surface tailored fungal biomass for the elimination of toxic dye from wastewater, Int. J. Environ. Anal. Chem. 00 (2020) 1–16. https://doi.org/10.1080/03067319.2020.1787400

[50] M.M.A. El-Latif, A.M. Ibrahim, M.F. El-Kady, Adsorption equilibrium, kinetics and thermodynamics of methylene blue from aqueous solutions using biopolymer oak sawdust composite, J. Am. Sci. 6 (2010) 267–283.

[51] F.Huang, P.M. Singh, A.J. Ragauskas, Characterization of milled wood lignin (MWL) in loblolly pine stem wood, residue, and bark, J. Agric. Food Chem. 59 (2011) 12910–12916. https://doi.org/10.1021/jf202701b

[52] S. Wang, B. Ru, H. Lin, W. Sun, Z. Luo, Pyrolysis behaviors of four lignin polymers isolated from the same pine wood, Bioresour. Technol. 182 (2015) 120–127. https://doi.org/10.1016/j.biortech.2015.01.127

[53] F. Taleb, M. Ammar, M. ben Mosbah, R. ben Salem, Y. Moussaoui, Chemical modification of lignin derived from spent coffee grounds for methylene blue adsorption, Sci. Rep. 10 (2020) 1–13. https://doi.org/10.1038/s41598-020-68047-6

[54] C.F. Lima, L.C.A. Barbosa, M.N.N. Silva, J.L. Colodette, F.O. Silvério, In situ determination of the syringyl/guaiacyl ratio of residual lignin in pre-bleached eucalypt kraft pulps by analytical pyrolysis, J. Anal. Appl. Pyrolysis. 112 (2015) 164–172.

https://doi.org/10.1016/j.jaap.2015.02.002

[55] C. Liu, Y. Deng, S. Wu, H. Mou, J. Liang, M. Lei, Study on the pyrolysis mechanism of three guaiacyl-type lignin monomeric model compounds, J. Anal. Appl. Pyrolysis. 118 (2016) 123–129. https://doi.org/10.1016/j.jaap.2016.01.007

[56] M. Agustí, V. Almela, M. Juan, F. Alferez, F.R. Tadeo, L. Zacarías, Histological and physiological characterization of rind breakdown of "Navelate" sweet orange, Ann. Bot. 88 (2001) 415–422. https://doi.org/10.1006/anbo.2001.1482

[57] M.E. Fernandez, G.V. Nunell, P.R. Bonelli, A.L. Cukierman, Activated carbon developed from orange peels: batch and dynamic competitive adsorption of basic dyes, Ind. Crops Prod. 62 (2014) 437–445. https://doi.org/10.1016/j.indcrop.2014.09.015

[58] M. Poletto, Thermal degradation and morphological aspects of four wood species used in lumber industry, Rev. Árvore. 40 (2016) 941–948. https://doi.org/10.1590/0100-67622016000500018

[59] F.C. Beall, H.W. Eilckner, Thermal degradation of wood components, U.S.D.A. For. Serv. Res. Pap. 130 (1970).

[60] B.L.C. Pereira, A. de C.O. Carneiro, A.M.M.L. Carvalho, P.F. Trugilho, I.C.N.A. Melo, A.C. Oliveira, Estudo da degradação térmica da madeira de Eucalyptus através de termogravimetria e calorimetria, Rev. Arvore. 37 (2013) 567–576. https://doi.org/10.1590/S0100-67622013000300020

[61] M. Thommes, K. Kaneko, A.V. Neimark, J.P. Olivier, F. Rodriguez-Reinoso, J. Rouquerol, K.S.W. Sing, Physisorption of gases, with special reference to the evaluation of surface area and pore size distribution (IUPAC Technical Report), Pure Appl. Chem. 87 (2015) 1051–1069. https://doi.org/10.1515/pac-2014-1117

[62] S. Naumov, R. Valiullin, J. Kärger, Adsorption hysteresis phenomena in mesopores, Diffus. Fundam. 6 (2007) 67.1–67.2.

[63] W. Li, Q. Yue, B. Gao, X. Wang, Y. Qi, Y. Zhao, Y. Li, Preparation of sludge-based activated carbon made from paper mill sewage sludge by steam activation for dye wastewater treatment, Desalination. 278 (2011) 179–185. https://doi.org/10.1016/j.desal.2011.05.020

[64] P. Chand, A.K. Shil, M. Sharma, Y.B. Pakade, Improved adsorption of cadmium ions from aqueous solution using chemically modified apple pomace: mechanism, kinetics, and thermodynamics, Int. Biodeterior. Biodegradation. 90 (2014) 8–16. https://doi.org/10.1016/j.ibiod.2013.10.028

[65] A. Klapiszewski, M. Wysokowski, I. Majchrzak, T. Szatkowski, M. Nowacka, K.S.N.

N, K. Szwarc-rzepka, P.B. Bartczak, H. Ehrlich, T. Jesionowski, Preparation and characterization of multifunctional chitin/lignin materials, J. Nanomater. 2013 (2013) Article ID 425726. https://doi.org/10.1155/2013/425726

[66] B. Raij, Determinação do ponto de carga zero em solos, Bragantia. 32 (1973) 337–347. https://doi.org/10.1590/S0006-87051973000100018

[67] N.K. Mall, I. D., Srivastava, D. C., Agarwal, Removal of orange-G and methyl violet dyes by adsorption onto bagasse fly ash-kinetic study and equilibrium isotherm analyses, Dye. Pigment. 69 (2006) 210–223. https://doi.org/10.1016/j.dyepig.2005.03.013

[68] M. Suzuki, Adsorption Engineering, Japan, 1990.

[69] M. Chairat, J.B. Bremner, K. Chantrapromma, Dyeing of cotton and silk yarn with the extracted dye from the fruit hulls of mangosteen, Garcinia mangostana Linn, Fibers Polym. 8 (2007) 613–619. https://doi.org/10.1007/BF02875998

[70] R. Scotti, E.C. Lima, E.V. Benvenutti, C.M.S. Piatnicki, Y. Gushikem, Azul de metileno imobilizado na celulose/TiO_2 e SiO_2/TiO_2: propriedades eletroquímicas e planejamento fatorial, Quim. Nova. 29 (2006) 208–212. https://doi.org/https://doi.org/10.1590/S0100-40422006000200006

[71] V.K. Garg, R. Gupta, A.B. Yadav, R. Kumar, Dye removal from aqueous solution by adsorption on treated sawdust, Bioresour. Technol. 89 (2003) 121–124. https://doi.org/10.1016/S0960-8524(03)00058-0

[72] L.R. Bonetto, F. Ferrarini, C. De Marco, J.S. Crespo, R. Guégan, M. Giovanela, Removal of methyl violet 2B dye from aqueous solution using a magnetic composite as an adsorbent, J. Water Process Eng. 6 (2015) 11–20. https://doi.org/10.1016/j.jwpe.2015.02.006.

[73] N. Ali, A. Hameed, S. Ahmed, Physicochemical characterization and bioremediation perspective of textile effluent, dyes and metals by indigenous bacteria, J. Hazard. Mater. 164 (2009) 322–328. https://doi.org/10.1016/j.jhazmat.2008.08.006.

[74] W. Zou, H. Bai, S. Gao, K. Li, Characterization of modified sawdust, kinetic and equilibrium study about methylene blue adsorption in batch mode, Korean J. Chem. Eng. 30 (2013) 111–122. https://doi.org/10.1007/s11814-012-0096-y

[75] K. Fu, Q. Yue, B. Gao, Y. Sun, L. Zhu, Preparation, characterization and application of lignin-based activated carbon from black liquor lignin by steam activation, Chem. Eng. J. 228 (2013) 1074–1082. https://doi.org/https://doi.org/10.1016/j.cej.2013.05.028

[76] V. Ponnusami, S. Vikram, S.N. Srivastava, Guava (Psidium guajava) leaf powder:

novel adsorbent for removal of methylene blue from aqueous solutions, J. Hazard. Mater. 152 (2008) 276–286. https://doi.org/10.1016/j.jhazmat.2007.06.107

[77] W. Plazinski, W. Rudzinski, A. Plazinska, Theoretical models of sorption kinetics including a surface reaction mechanism: a review, Adv. Colloid Interface Sci. 152 (2009) 2–13. https://doi.org/10.1016/j.cis.2009.07.009

[78] M. Doğan, M. Alkan, A. Türkyilmaz, Y. Özdemir, Kinetics and mechanism of removal of methylene blue by adsorption onto perlite, J. Hazard. Mater. 109 (2009) 2–13. https://doi.org/10.1016/j.jhazmat.2004.03.003

[79] G. Akkaya, F. Güzel, Application of some domestic wastes as new low-cost biosorbents for removal of methylene blue: kinetic and equilibrium studies, Chem. Eng. Commun. 201 (2014) 557–578. https://doi.org/10.1080/00986445.2013.780166

[80] M.A. Kumar, R.; Barakat, Decolourization of hazardous brilliant green from aqueous solution using binary oxidized cactus fruit peel, Chem. Eng. J. 226 (2013) 377–383. https://doi.org/10.1016/j.cej.2013.04.063

[81] A. Dąbrowski, Adsorption — from theory to practice, Adv. Colloid Interface Sci. 93 (2001) 135–224. https://doi.org/https://doi.org/10.1016/S0001-8686(00)00082-8

[82] G.D. Değermenci, N. Değermenci, V. Ayvaoğlu, E. Durmaz, D. Çakır, E. Akan, Adsorption of reactive dyes on lignocellulosic waste; characterization, equilibrium, kinetic and thermodynamic studies, J. Clean. Prod. 225 (2019) 1220–1229. https://doi.org/https://doi.org/10.1016/j.jclepro.2019.03.260

[83] H. Allidadi, M. Dolatabi, M. Davoud, F. Barjasteh-Askari, F. Jamali-Behnam, A. Hosseinzadeh, Enhanced removal of tetracycline using modified sawdust: optimization, isotherm, kinetics, and regeneration studies, Process Saf. Environ. Prot. 117 (2018) 51–60. https://doi.org/10.1016/j.psep.2018.04.007

[84] Z. Yaneva, N. Georgieva, Insights into congo red adsorption on agro-industrial materials- spectral, equilibrium, kinetic, thermodynamic, dynamic and desorption studies. A review, Int. Rev. Chem. Eng. 4 (2012) 127–146.

[85] C. Vimonses, V.; Jin, B.; Chow, C.W.K.; Saint, Enhancing removal efficiency of anionic dye by combination and calcination of clay materials and calcium hydroxide, J. Hazard. Mater. 171 (2009) 941–947. https://doi.org/10.1016/j.jhazmat.2009.06.094

[86] J. Gómez-pastora, E. Bringas, I. Ortiz, Recent progress and future challenges on the use of high performance magnetic nano-adsorbents in environmental applications, Chem. Eng. J. 256 (2014) 187–204. https://doi.org/10.1016/j.cej.2014.06.119

FIGURE CAPTIONS

Figure 1. FT-IR spectra of the *E. grandis* lignin **(a)** before and **(b)** after MB adsorption

Figure 2. Solid-state ^{13}C NMR spectrum of *E. grandis* lignin

Figure 3. Pyrogram of *E. grandis* lignin

Figure 4. FESEM images of *E. grandis* lignin with magnification levels of **(a)** 500 × and **(b)** 2000 ×

Figure 5. TG and DTG curves of the *E. grandis* lignin

Figure 6. N_2 adsorption and desorption isotherms for *E. grandis* lignin

Figure 7. Determination of the pH_{PZC} of *E. grandis* lignin. Experimental conditions: pH = 2.0-11.0; lignin dosage = 100 mg; temperature = 25 °C; and contact time = 24 h

Figure 8. Influence of the *E. grandis* lignin dosage on the MB removal. Experimental conditions: pH = 5.6; stirring intensity = 150 rpm; temperature = 25 °C; contact time = 8 h; and MB concentration = 100 mg L^{-1}

Figure 9. Effect of the stirring frequency on the MB removal. Experimental conditions: pH = 5.6; lignin dosage = 225 mg; temperature = 25 °C; contact time = 8 h; and MB concentration = 100 mg L^{-1}

Figure 10. Effect of initial pH on the MB removal. Experimental conditions: stirring frequency = 150 rpm; lignin dosage = 225 mg; temperature = 25 °C; contact time = 8 h; and MB concentration = 100 mg L^{-1}

Figure 11. Chemical structure of MB as a function of pH

Figure 12. Experimental data adjusted to the Freundlich, Langmuir, Temkin and Dubinin-Radushkevich isotherms

Figure 13. Possible interactions between the MB molecules and *E. grandis* lignin

Figure 14. Reuse of the *E. grandis* lignin. Experimental conditions: C_0 = 100 mg L^{-1}; m = 225 mg; v = 150 rpm; t = 8 h; and T = 25°C

Figure 15. *Eucalyptus grandis* lignin appearance: **(a)** before and **(b)** after the first desorption

TABLE CAPTIONS

Table 1. Separation factor and types of isotherms

Table 2. Results of the elemental analysis for *E. grandis* lignin

Table 3. Assignments of the main peaks observed in the FT-IR spectrum of *E. grandis* lignin before MB adsorption

Table 4. Pyrolysis products identified in the pyrogram of *E. grandis* lignin

Table 5. Specific surface areas of various lignin samples

Table 6. Parameters obtained from the Freundlich, Langmuir, Temkin and Dubinin-Radushkevich isotherm models and the *Fisher* test

Table 7. Comparison with modified and native lignins in terms of q_m values and operational conditions for MB adsorption

Table 8. Kinetic parameters for the nonlinear pseudo-first- and pseudo-second-order models

Table 9. Thermodynamic parameters for MB removal

Author contributions

Use this form to specify the contribution of each author of your manuscript. A distinction is made between five types of contributions: Conceived and designed the analysis; Collected the data; Contributed data or analysis tools; Performed the analysis; Wrote the paper.

For each author of your manuscript, please indicate the types of contributions the author has made. An author may have made more than one type of contribution. Optionally, for each contribution type, you may specify the contribution of an author in more detail by providing a one-sentence statement in which the contribution is summarized. In the case of an author who contributed to performing the analysis, the author's contribution for instance could be specified in more detail as 'Performed the computer simulations', 'Performed the statistical analysis', or 'Performed the text mining analysis'.

If an author has made a contribution that is not covered by the five pre-defined contribution types, then please choose 'Other contribution' and provide a one-sentence statement summarizing the author's contribution.

Abstract

A lignin sample was extracted from *Eucalyptus grandis* sawdust, by the Klason method, and used as adsorbent for the removal of methylene blue (MB) from aqueous solutions. By using a set of complementary analytical tools, the lignin appeared to be constituted of oxygenated functional groups and aromatic moieties, while showing a specific surface area of 20 m^2 g^{-1} and polydisperse particles. Different experimental conditions with various solid to liquid ratio, pH, as well as other external experimental parameters were investigated for the removal of MB by the lignin sample. The experimental adsorption data at the equilibrium were properly fitted by Langmuir model, while adsorption kinetical isotherms were correctly adjusted by the pseudo-second order model. The MB removal by lignin was spontaneous involving physisorption mechanisms leading to a saturation of the adsorption sites with a maximum adsorbed amount of about 32 mg g^{-1}. The data acquired in this study also emphasized the interests to use lignin as potential adsorbent in the light of its properties for the removal of cationic dyes, including MB, with possible recycling and reuse cycles of lignin without any significant loss of its properties.

Keywords: *Eucalyptus grandis* lignin; methylene blue; adsorption.

Graphical abstract